ELECTROHYDRODYNAMIC CONDUCTION PUMPING IN MICRO-SCALE WITH TWO PHASE FLOW

A Major Qualifying Project

Submitted to the

Department of Mechanical Engineering

in Partial Fulfillment of the Requirements for the Degree of

Bachelor of Science in Mechanical Engineering at the

Worcester Polytechnic Institute

March 2016

Ahmed Safat Hossain

Darien Nate Khea

Dr. Jamal Seyed-Yagoobi

Professor of Mechanical Engineering

Project Advisor

Abstract

The heat transfer requirements in order to regulate operating temperatures in high power electronics stems from the technological advancements of miniaturizing systems. Traditional coolant pumps, which have moving parts, do not provide cooling solutions in micro-scale due to complex designs. Electrohydrodynamic (EHD) conduction pumps can be utilized for micro-scale thermal control. The phenomenon of EHD conduction occurs when dissociated electrolyte constituents in a dielectric fluid interact with an applied electric field. This allows a net force in the working fluid, which provides a net flow in a particular direction. EHD conduction pumps are advantageous in the sense that they are simple in design, have no moving parts, require lower power to operate, and is able to be used in microgravity. There are previous experiments that prove that effective heat transfer enhancement in single phase can be achieved for systems in both macro- and meso- scales. This project offers performance characteristics such as pressure and flow rate generation in micro-scale for a single phase flow based on an EHD pump consisting of three electrode pairs. These electrode pairs comprise of a flush ring ground electrode and two 400 micron perforated high voltage electrodes. The working fluid was chosen to be HCFC-123 that operated within an ambient environment.

Acknowledgements

Table of Contents

Table of Figures

Tables of Tables

Chapter 1 – Introduction

1.1 Introduction to EHD Pumping

Electrohydrodynamics (EHD) studies the interactions between an applied electrical field and any resulting fluid flow. In the presence of an electric field, a set of EHD forces resulting from the presence of charged elements in the fluid will cause fluid motion. This gives the EHD its most valuable application, EHD pumping. The three major types of EHD pumping driven by Coulomb Force are conduction, induction, and ion drag, the modifications between which is the procedure used to produce charges in the fluid. Conduction has just been of greater interest in recent years because it is reliable and simpler than the other types listed. One important use that has been previously demonstrated for EHD pumping is to improve heat transfer capabilities [7]. A system consisting of the pump and fluid circulation can allow the fluid to carry away heat produced from an operating electronic or piece of hardware cooling it down. Other uses involve terrestrial applications, in high power electronics cooling, and for aerospace, because EHD works in zero gravity [8] and has low mass designs with no moving parts.

The purpose of this Major Qualifying Project was to take the EHD Pumping concept in mind and to take the pump to micro-scale to study the magnified effects on heat transfer. The effects will be compared to EHD Pumps run in Meso Scale to understand the improved efficiency [4]. To show the effective generation of flow and pressure of the fluid, a complete loop was assembled using a complex system of sensors and data acquisition modules. This report underlines the entire design, fabrication and testing and provides research to study the improved performance of a Micro-scale EHD Pump. The conclusions from this study could be directly applied to solve a wide range of fundamental problems in the engineering industry.

1.2 Overview of EHD pumping

The EHD phenomena involve the interaction of electric fields and flow fields in a fluid medium. Three forces are present in this interaction: Coulomb, Dielectrophoretic, and Electrostriction, as shown as three terms respectively in this equation [13]:

$$\vec{F}_e = q\vec{E} - \frac{1}{2}E^2\nabla\epsilon + \nabla\left[\rho\frac{E^2}{2}\left(\frac{\partial\epsilon}{\partial\rho}\right)_T\right]$$

For an isothermal, incompressible dielectric fluid medium, the Coulomb force is solely responsible for flow generation in EHD pumping [3].

1.3 Types of EHD Pumping

ION DRAG

Among the complex phenomena of EHD Pumping, Ion Drag is one of the primary and earliest found methods to successfully create fluid flow with net charge distribution. Ion-drag EHD pump uses the interaction of an electric field with electric charges, dipoles or particles injected

from the emitter in a fluid in order to generate a net flow (Fig. 1) [7]
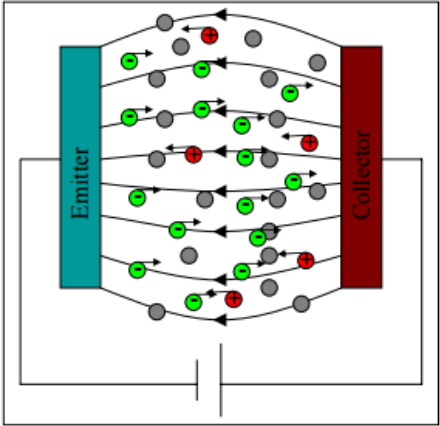
Fig.1: Ion-Drag pumping mechanism [7]
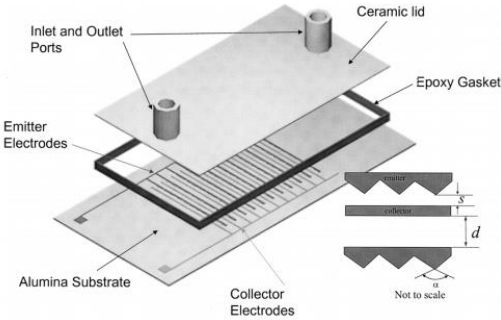
Fig 2: Ion Drag Design [7]

In the Ion Drag design (Fig 2), injection of ions in the working fluid come from the emitter using the Corona discharge effect. Free charge will drag the adjacent fluid along electric field lines. The primary reason, it is not the preferred method of pumping is because of deterioration of the fluid's electrical properties because of the charges being pumped into it. Electrical conductivity in a fluid is a measure of how many charge carriers there are and the relative speed

of their flow. This is effected in Ion drag pumping. Also that data cannot be very reliable since operation may be inconsistent.

INDUCTION

The concept of Induction pumping comes from charges induced in a liquid caused by a gradient or discontinuity of the electrical conductivity. Often an AC traveling electric wave attracts or repels these induced charges which causes the motion in the working fluid. The electric wave is controlled by varying voltage and frequency. The rate of heat transfer is directly related to the combination of heat flux and voltage. For alternate conditions between heat flux and voltage, the frequency determines the heat transfer rate. The disadvantages for this method are High power consumption and a Complex Design Structure. So it is not the ideal method in running Micro-scale EHD Pumping experiments [10]

CONDCUTION

The interface between electric fields and dissociated ionic charges in dielectric fluids is referred to as EHD conduction pumping. In EHD conduction pumping, when an electric field is applied to a fluid, dissociation and recombination of electrolytic species produces heterocharge layers in the vicinity of electrodes. Attraction between electrodes and heterocharge layers induces a fluid motion and a net flow is generated if the electrodes are properly designed [3]. At high electric fields, the rate of dissociation exceeds the rate of recombination. A heterocharge layer is where the dissociation-recombination reactions is not in equilibrium. Oppositely charged ions are attracted to oppositely charged electrodes (ground and high voltage). This exerts a force on the fluid for each ionic species (positive and negative). For symmetric electrodes these forces

will cancel each other out. Net flow is generated when the electrode geometry allows for a net force in the desired flow direction.
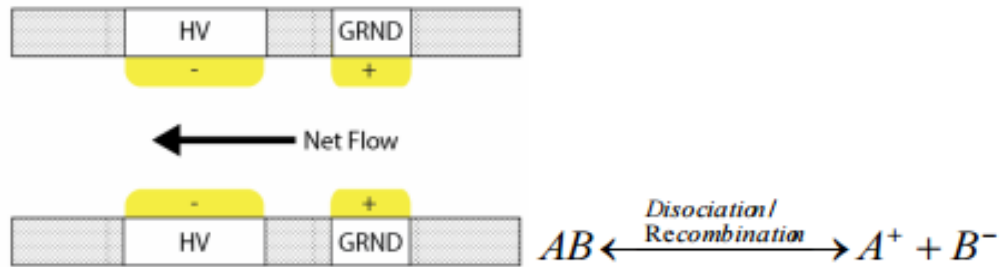
Fig 3: Molecular Dissociation/Recombination and net flow [4]

1.4 Applications of EHD Pumping

There are a number of advantages to EHD conduction pumping with regards to mass transport (control and distribution) and effective heat transfer. This allows it to be used in multiple applications across various engineering industries. Some the advantages include [2]:

a) Non-mechanical (no moving parts)

b) Lightweight

c) Low noise

d) Suitable for special environments (e.g. space)

e) Applicable for single and multiphase flows

f) Ability to enhance control of fluid using electric fields

The key advantage to EHD conduction pumping is its flexibility. The EHD conduction pumping phenomenon is receptive, i.e. pumping changes almost immediately when changing the forced electric field. Most fluids in thermal systems, namely refrigerants, happen to be dielectrics, which makes flow distribution and control in thermal systems using EHD conduction

pumps entirely achievable. Although with all these benefits in hand, the high voltage

requirement makes EHD pumps dangerous to operate.

The above following properties have allowed EHD conduction technology to improve the

heat transport properties of cooling systems that use refrigerants [11]. The Non-mechanical

system combined with the lightweight property have made EHD conduction pumping an

attractive technology in space environments since it can work under microgravity conditions [8]

and other applications (see Fig. 4). EHD conduction pumping can also successfully pump thin

fluid films, which can be used to pump vapor phases that can be carried by an EHD driven liquid

phase [12]. As a relatively new field, it is also developing to reach the technology for use in

autonomous actuation [5].
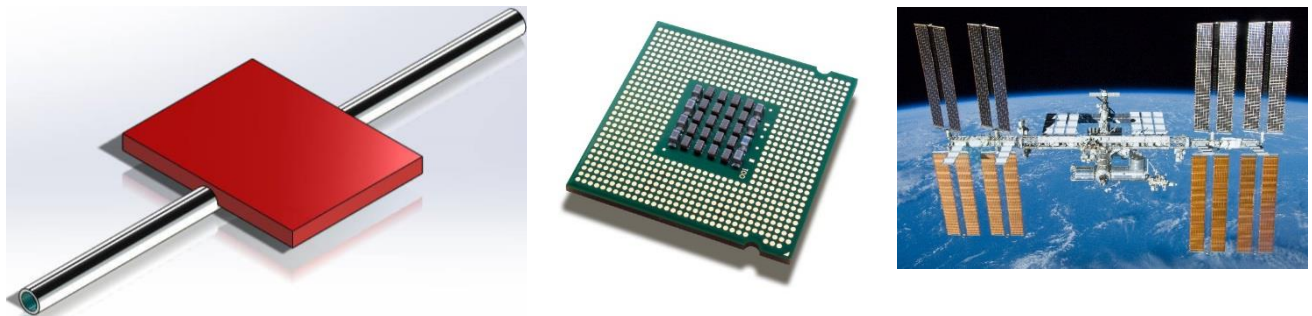
Fig 5: Applications of EHD Conduction Pumping

1.5 Operating Conditions and Goals in EHD Pumping Experiments

The goal of this project was to characterize the performance of an innovative, micro scale

EHD conduction pump for heat transfer enhancement in single and two-phase flows. For this

purpose an experimental setup had to be constructed to test the pressure and flow rate generation

capabilities of the micro scale pump. The experimental setup was a loop similar to HVAC

systems [reference], which includes an evaporator section to heat the fluid and a condenser section to cool the fluid back to single phase so it can be circulated back into the evaporator.

To run an experiment involving an EHD conduction pump, the primary variable to take into concern, the nominal electric field strength. For EHD conduction to work this field strength cannot exceed the dielectric strength of the working fluid (given in volts per some gap in mm), but must still be on the order of 10^6 V/m. The nominal field is the voltage supplied to the pump times the gap distance between the high voltage and ground electrodes. For a micro scale EHD conduction pump, the allowable voltage magnitude is directly related to the gap between the electrodes. The electrodes themselves can have many shapes, as illustrated below [12]:
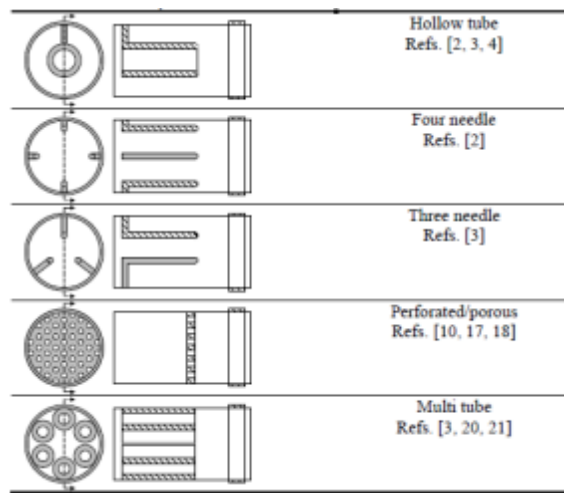
Figure 6: Different Electrode Geometries [12]

For this project, the allowable range theoretically set to run the high voltage electrode for EHD conduction pump was within 700V-1200V. This was decided from a comparison based on the ratio of values from the meso scale experiment to study EHD conduction pumping. The performance curve to study mass flow rate, differential pressure and heat transfer was all done based within the range provided above. The purpose of the experimental setup was to use input voltages to the EHD conduction pump and heater to generate flow and control the vapor quality,

and measure the resulting pressure and flow rate at different voltage and quality levels. Due to time constraints, data for single and two phase flow could not be obtained. Therefore this report details the design and construction efforts only.

For any EHD conduction pump in a loop experiment, the primary goal is to use the pump to successfully create a complete circulation of the fluid in the loop. This can only be possible by creating a sustainable change in pressure between the electrodes in the pump. This pressure gain must be higher that the pressure loss due to friction and resistance along the loop. For a micro scale pump, the pressure gain is not significant enough. As a result, the pressure loss must be kept to a minimal value. For two phase operations, characterization of a successful operation with evaporation based on vapor quality is the goal. For both single phase and two phase operations, the saturated temperature and saturated pressure control is an essential step to calculate. EHD conductions use very small currents so even though they require high voltages, the overall power consumption is very low. Fully capturing the performance of the micro-scale pump will provide in-depth knowledge of how EHD conduction can control single and two-phase flows at such a small scale for future studies

1.6 Microscale EHD Pump

The experimental study to be performed using the experimental setup detailed in this report will observe the central behavior and performance of EHD conduction pumping at the micro scale where the single-phase flow and pressure generation of the pump will be characterized. The EHD pumping of single phase flow in micro-channel in the presence of heat transfer will also be studied and the enhancement of heat transfer due to the EHD conduction pump will be quantified. The primary reasons for studying micro scale EHD conduction pumping is that thermal conductivity is increased for reduced area. This is because increased ratio between

surface area and volume, which is achieved by reducing the characteristic size of the flow

channels:

$$k = \frac{Q\Delta x}{A(T_2 - T_1)}$$

Along with this, lower voltages can be applied to the EHD conduction pump to achieve the

required electric field strength. This is possible since the distance between the electrodes in the

pump is very small. The lower voltage low current used therefore results lower power

consumption. This creates an ideal technology that can be applied to multiple aspects of the

engineering industry. The change of scale from meso to micro generates significant pressure and

flowrates allowing enhanced fluid circulation and heat transfer [3]. Due to specific

environmental requirement needs for any given engineering system, micro scale pumps

producing low noise and low vibration makes EHD conduction pumps an attractive piece of

instrument to be used.

The micro scale pump design for our experiment consisted of a pump with two high voltage and

two ground voltage electrodes, with an additional electrode pair downstream with a high voltage

electrode embedded in an evaporator for phase change. The space between each high voltage and

ground electrode was 1 mm. The tube that allows the fluid to flow through the pump is

approximately 1mm in diameter. As shown in Fig. 8, the 3d model of the EHD Pump and

evaporator is displayed:
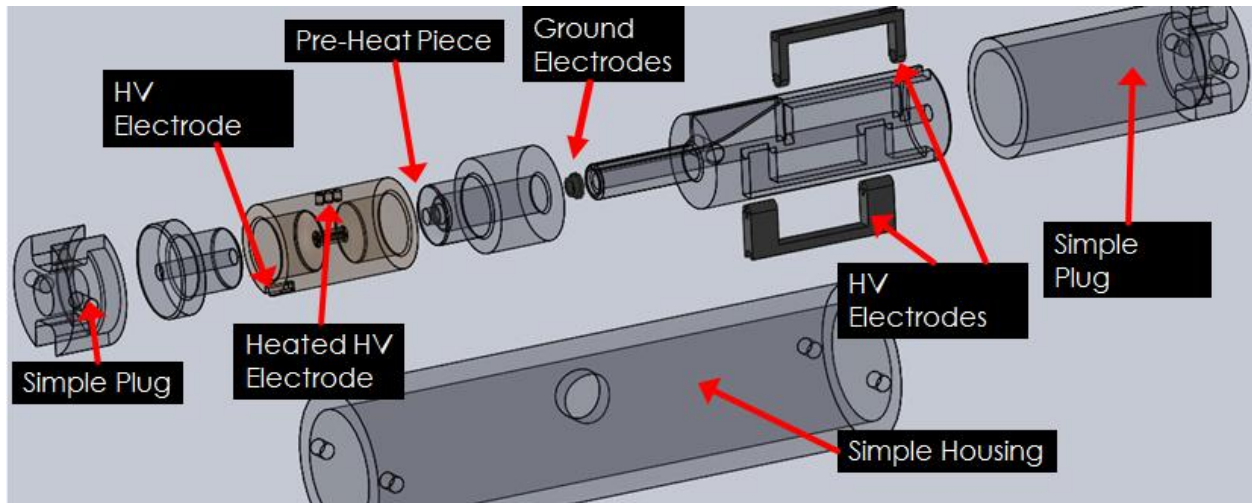
Fig 7: 3D Model of Micro-Scale EHD Pump and Evaporator

The big housing tube on the bottom of this image is exactly 60mm long

The pump was designed with a simple housing, shown on the bottom in Fig 8. to hold the individual components in it. It was then closed from both ends to ensure the pump will not come apart during operation. The wiring for the High Voltage and ground electrodes were separately pulled out and connected to a power supply. Fig. 6 shows the actual model of the pump installed into the loop. This pump was design in collaboration with the NASA Goddard Space Flight Center, and that the pieces were manufactured there and assembled at WPI.

Fig 8: Micro-scale EHD Pump and Evaporator

The voltage set for the heater was only set to create a pressure differential in the evaporator next to the pump to create a higher flow rate and study different flow rate based heat transfer only for single phase. To maintain a proper standard for a fluid conditions, a Saturation Temperature and Pressure must be set from the reservoir. This provides the exact boiling point of the fluid at that corresponding temperature and pressure to carry out single and two phase experiments. Other variables include a needle valve in the loop to vary the flow rate in the system and multiple ball vales to isolate certain portions of the circulation to study static and dynamic pressure values.

Chapter 2 – Theoretical Calculations

Preliminary calculations for the amount of pressure generation and pressure loss experienced in a system in both single and two phase flows are significant before designing the experimental loop. The pressure generation occurs in the pump and in the evaporator, which are both located within an integrated housing. Pressure losses arise at any location where the

working fluid is flowing. For a two phase experiment, it is necessary to calculate the amount of power applied to evaporator for a phase change. In order to achieve subcooling conditions of the working fluid, an additional calculation must be made to solve for the length of a condenser.

2.1 EHD Pump Performance Estimates

In single phase, theoretical calculations for pressure generation in the test loop rely on various parameters. The pressure generation calculation is based on a previous experiment conducted in 2004 by Yinshan Feng and Jamal Seyed-Yagoobi on "understanding [the] electrohydrodynamic conduction pumping phenomenon." The principle equation that was used is shown below:

$$\Delta P_{generation} = (0.85c)m\epsilon\frac{V^2}{d^2}$$

Where c is a constant based on the closeness of the electrode, m is the number of electrode pairs, ϵ is the permittivity of the working fluid (HCFC-123), V is the applied voltage, and d is the distance between electrode pairs. The openness of the electrodes was calculated to be approximately 31.25%, which constitutes a closeness of 68.75%. It is important to note that there are separate voltage sources for the pump and the evaporator although they are within an integrated configuration. Different pressure generations will arise from the different applied voltages. In the pump setup, as previously mentioned, there are two electrode pairs whereas in the evaporator section, there is only one electrode pair. The resulting pressure generation, with varying voltages, for each section of the setup is shown in the graph below:

Theoretical Pressure Generation With Varying Voltages
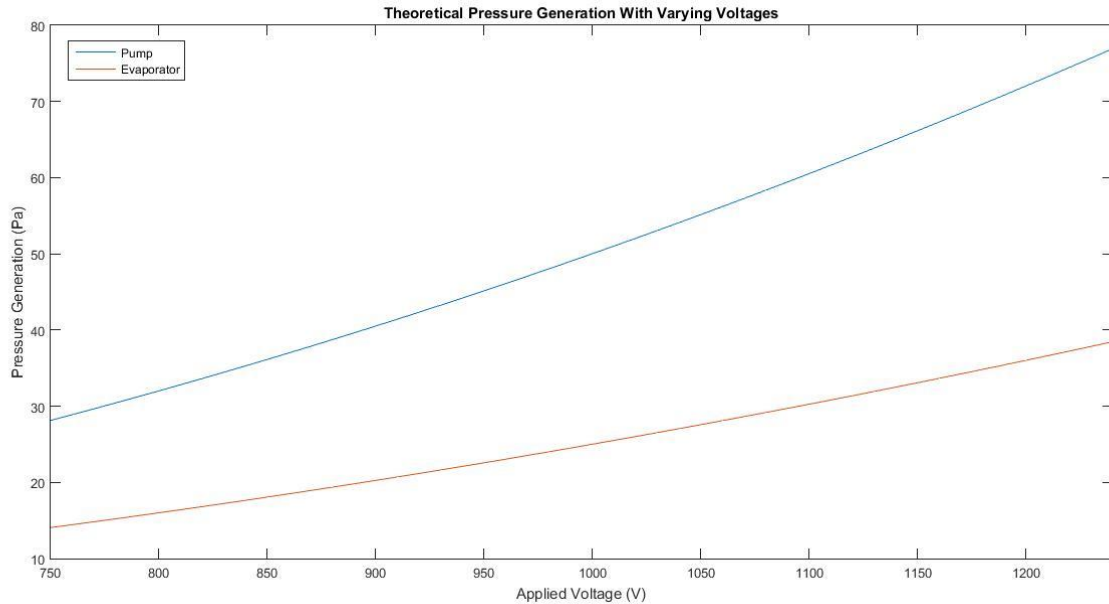
From theoretical calculations, the pressure generation at the maximum applied voltage of 1240 V for the pump and evaporator are approximately 77 Pa and 38.5 Pa, respectively.

Since there are issues with the previous pressure generation equation, which assumes an ideal set of conditions, better estimates are provided when analyzing previous experimental values. The analysis was broken down into how much pressure that each electrode pair was capable of generating. This was done in order to better compare data to other experiments that may have greater or fewer number of electrode pairs. One experiment, conducted by Lei Yang, used a macro-scale 10 electrode, perforated pump at 10 kV. The second experiment, conducted by Viral Patel, used a meso-scale 20 electrode, flush ring pump at 1 kV. Shown below are two tables summarizing each pump's pressure generation (P) and corresponding flow rate (F):
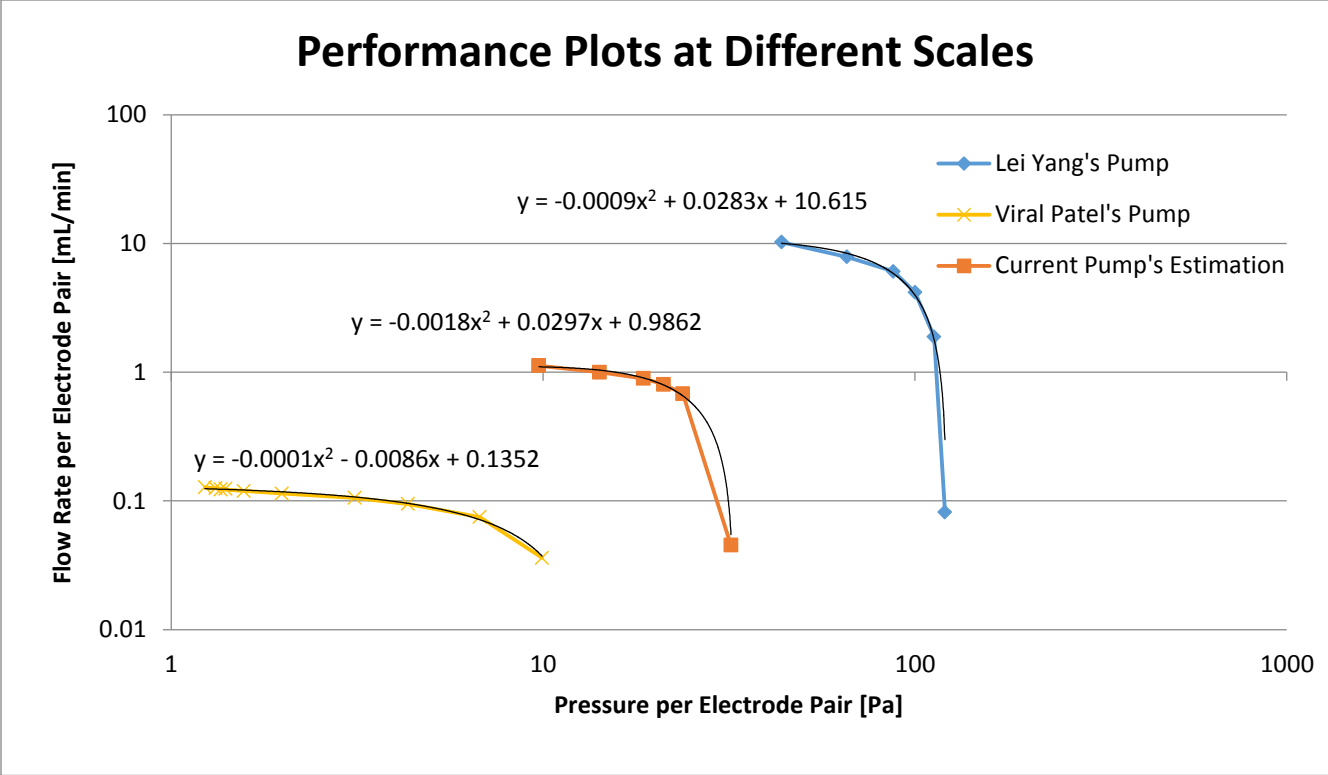
Total P (Pa)	P Per Pair (Pa)	Total F (mL/min)	F Per Pair (mL/min)
437.5	43.75	102.5	10.25
656.2	65.62	78.7	7.87
875	87.5	60.7	6.07

1000	100	41.8	4.18
1125	112.5	18.8	1.88
1203	120.3	0.82	0.082

Total P (Pa)	P Per Pair (Pa)	Total F (mL/min)	F Per Pair (mL/min)
39.68	1.984	2.284	0.1142
62.26	3.113	2.115	0.1058
86.52	4.326	1.896	0.0948
135.0	6.752	1.499	0.0750
198.6	9.930	0.723	0.0362
216.2	10.81	0.0473	0.0024

In order to generate a pressure generation curve for the current pump configuration, it is compared to both previous experiments based on how closely related they are to one another. The majority of characteristics for the current pump, which includes operating voltage, size of pump, predicted pressure and flow rate ranges, can be attributed to Viral's meso-scale pump. The only difference is that the current pump uses a perforated pump as seen in Lei's experiment rather than the flush ring pump seen in Viral's experiment. Based on weighted slopes of curves and characteristics of the pumps, a graph shown below displays the current pump's pressure generation curve alongside curves of previous experiments:

Performance Plots at Different Scales

$y = -0.0009x^2 + 0.0283x + 10.615$

$y = -0.0018x^2 + 0.0297x + 0.9862$

$y = -0.0001x^2 - 0.0086x + 0.1352$

- ◆ Lei Yang's Pump
- ✕ Viral Patel's Pump
- ■ Current Pump's Estimation

Flow Rate per Electrode Pair [mL/min]

Pressure per Electrode Pair [Pa]

Based on the estimated curve of the current pump, a table shown below better displays

the numerical values of the pump's pressure generation (P) and corresponding flow rate (F):

Total P (Pa)	P Per Pair (Pa)	Total F (mL/min)	F Per Pair (mL/min)
29.2	9.73	3.37	1.12
42.5	14.2	3.00	1.00
55.9	18.6	2.68	0.895
63.3	21.1	2.41	0.804
71.3	23.8	2.04	0.680
96.0	32.0	0.14	0.045

Compared to the previous maximum pressure generation of 115.5 Pa, the newly estimated

maximum pressure generation value of 96 Pa is relatively lower.

2.2 Single Phase Pressure Loss Theoretical Calculations

In order to decide whether or not the pressure generation in the loop is significant, it is important to calculate the pressure loss in the loop. For a system that is purely in single phase, the pressure loss can be calculated using the Darcy-Weisbach equation shown below:

$$\Delta P_{loss} = \frac{fL\rho V^2}{2D}$$

Where f is the friction factor, L is the length of pipes in different sections of the loop, ρ is the density of the working fluid (HCFC-123), V is the fluid velocity, and D is the inner diameter of pipes. To calculate the total pressure loss in the system, the loop is broken into three sections consisting of the pump, evaporator, and remaining pipe. Shown below is a table summarizing the significant parameters in each section of the loop:

Section	Length (m)	Diameter (m)	Cross Sectional Area (m^2)
Pump	39.58 x 10^{-3}	1.61 x 10^{-3}	2.04 x 10^{-6}
Evaporator	11.46 x 10^{-3}	1.61 x 10^{-3}	2.04 x 10^{-6}
Remaining Pipe	3	4.57 x 10^{-3}	1.64 x 10^{-5}

A desired flow rate range is used to calculate the fluid velocity in sections of the loop with different diameters. Shown below is a table with various mass and volumetric flow rates, and the corresponding fluid velocity:

Section	Volumetric Flow rate (mL/min)	Mass Flow rate (kg/s)	Fluid Velocity (m/s)
Pump	0.1 – 5	2.43 x 10^{-6} - 1.22 x 10^{-4}	8.18 x 10^{-4} - 4.09 x 10^{-2}
Evaporator	0.1 – 5	2.43 x 10^{-6} - 1.22 x 10^{-4}	8.18 x 10^{-4} - 4.09 x 10^{-2}

Remaining Pipe	0.1 – 5	2.43 x 10^{-6} - 1.22 x 10^{-4}	1.02 x 10^{-4} - 5.10 x 10^{-3}

The last variable to account for is the friction factor, which can be calculated using the equation shown below:

$$f = \frac{64}{Re} \ with \ Re = \frac{\rho VD}{\mu}$$

Where Re is the Reynolds number, ρ is the density of the working fluid, V is the fluid velocity, D is the inner diameter of the pipes, and μ is the dynamic viscosity of the working fluid. The corresponding Reynolds numbers and friction factors for each section of the loop are shown below:

| Section	Reynolds Number	Friction Factor
Pump	4.7 – 235.5	13.6 – 0.27
Evaporator	4.7 – 235.5	13.6 – 0.27
Remaining Pipe	1.7 – 83.0	38.6 – 0.77

With all variables solved for, the pressure loss in each section of the loop can be calculated. These values are shown in the table below:

Section	Pressure Loss (Pa)
Pump	0.16 – 8.16
Evaporator	0.047 – 2.36
Remaining Pipe	0.19 – 9.52
Total System	0.40 – 20.0

Based on the theoretically calculated pressure generation and pressure loss values, the net pressure can be calculated using the equation:

$$`\Delta P_{net} = P_{pump} + P_{evaporator} - P_{loss}$$

Shown below is a graph depicting the net pressure as a function of the applied voltage:

Net Pressure With Varying Voltages
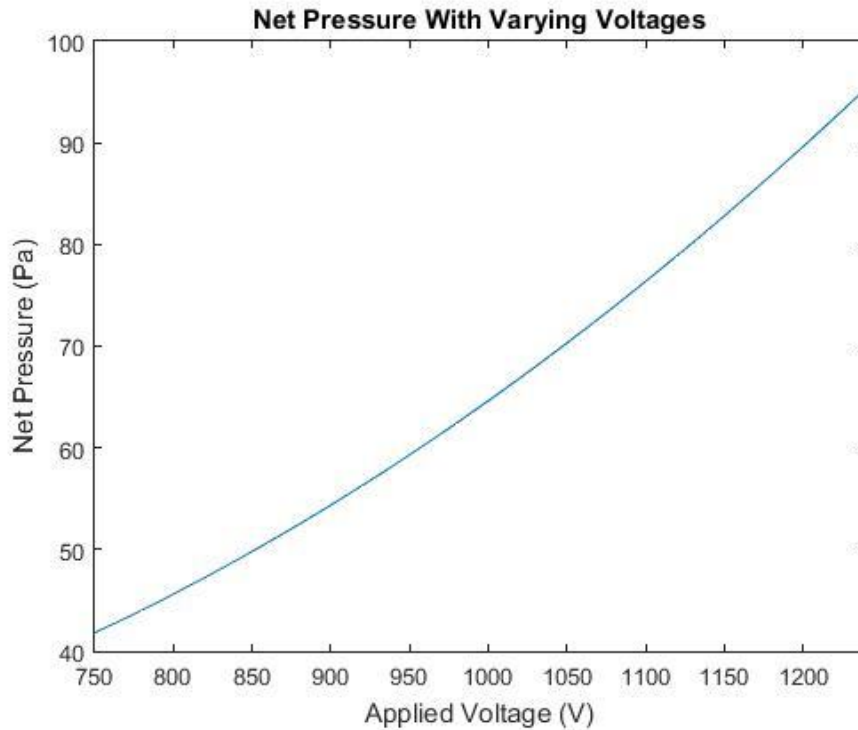
From theoretical calculations, the net pressure at the lowest applied voltage of 750 V is 41.8 Pa. In addition, the net pressure at the highest applied voltage of 1240 V is 95.3 Pa. It is important to note that these values are estimates, which inherently contain a 20% error.

2.3 Two Phase Pressure Loss Theoretical Calculations

In a two phase flow, the calculations for pressure loss are more extensive. This is due to separate calculations for liquid and vapor phases that exhibit turbulent flow in various sections of the loop. Based on the Reynolds number in single phase, it was valid to assume that laminar flow was only present. This assumption is no longer valid for a two phase experiment. To decide whether or not the pressure generation in the loop is significant for a two phase flow, it is important to calculate the experienced pressure loss. The equation for the total pressure loss in a system with two phases is shown below:

$$\Delta P_{total} = \Delta P_{static} + \Delta P_{momentum} + \Delta P_{frictional}$$

Static pressure losses can be ignored because the channels in the loop are assumed to be at the same height.

One way that pressure losses can arise in two phase flow is by momentum. The equation for this pressure loss is shown below:

$$\Delta P_{momentum} = G^2 \left\{ \left[\frac{(1-x)^2}{\rho_l(1-\epsilon)} + \frac{x^2}{\rho_g \epsilon} \right]_{outlet} - \left[\frac{(1-x)^2}{\rho_l(1-\epsilon)} + \frac{x^2}{\rho_g \epsilon} \right]_{inlet} \right\}$$

Where G is the mass flow rate flux, x is the vapor quality, ϵ is the drift flux void fraction, ρ_l is the density of the working fluid in the liquid phase, and ρ_g is the density of the working fluid in the gas phase. The equation for calculating the drift flux void fraction is shown below:

$$\epsilon = \frac{x}{\rho_g} \left[\left\{ (1 + 0.12(1-x)) \left(\frac{x}{\rho_g} + \frac{(1-x)}{\rho_l} \right) \right\} + \left\{ \frac{1.18(1-x)[g\sigma(\rho_l - \rho_g)]^{0.25}}{G\rho_l^{0.5}} \right\} \right]^{-1}$$

Where g is the acceleration due to gravity, σ is the surface tension of the working fluid, and all other variables were previously mentioned in the momentum pressure loss equation. The drift flux void fraction is used for separated flows due to different velocities in the liquid and gas phases in horizontal tubes.

Another way that pressure losses occur in two phase flow is by friction. The equation for this pressure loss is shown below:

$$\Delta P_{frictional-liquid} = 4f_l \left(\frac{L}{D} \right) \frac{G^2(1-x)^2}{2\rho_l}$$

$$\Delta P_{frictional-gas} = 4f_g \left(\frac{L}{D} \right) \frac{G^2(x)^2}{2\rho_g}$$

Where L is the length of the channel, D is the diameter where the fluid is exposed to, f_l is the friction factor of the liquid phase, f_g is the friction factor of the gas phase, and all other variables were previously mentioned in the momentum pressure loss equation. The friction factor in a two

phase flow is a conditional equation based on the flow regime that is present. This equation is

shown below:

$$
f_l \text{ or } f_g =
\begin{cases}
\dfrac{16}{Re_l \text{ or } Re_g} & Re_l \text{ or } Re_g < 1000 \\[2mm]
\dfrac{0.046}{\left(Re_l \text{ or } Re_g\right)^{0.2}} & Re_l \text{ or } Re_g > 2000 \\[2mm]
w\dfrac{16}{Re_l \text{ or } Re_g} + (1-w)\dfrac{0.046}{\left(Re_l \text{ or } Re_g\right)^{0.2}} & 1000 < Re_l \text{ or } Re_g < 2000
\end{cases}
$$

where:

$$
w = \frac{\left(Re_l \text{ or } Re_g - 1000\right)}{(2000 - 1000)}
$$

The equations for calculating the Reynolds number in the liquid or gas phase is shown below:

Gas phase:

$$
Re_g = \frac{GxD}{\mu_g}
$$

Liquid phase:

$$
Re_l = \frac{G(1-x)D}{\mu_l}
$$

Where μ_g is the viscosity of the working fluid in the gas phase, μ_l is the viscosity of the working

fluid in the liquid phase, and all other variables were previously mentioned. Once the frictional

pressure loss is calculated for, a corrective frictional pressure loss must be calculated as shown in

the equations below:

$$
\Delta P_{frictional-liquid-total} = \left(\Delta P_{frictional-liquid}\right)(\phi_l)
$$

$$
\Delta P_{frictional-gas-total} = \left(\Delta P_{frictional-gas}\right)(\phi_g)
$$

Where $\Delta P_{frictional-liquid}$ is the frictional pressure drop due to the liquid phase, $\Delta P_{frictional-gas}$ is the frictional pressure drop due to the gas phase, ϕ_l is the liquid multiplier, and ϕ_g is the gas multiplier. The liquid and gas multiplier can be calculated using the equations shown below:

Gas Multiplier:

$$\phi_g = 1 + C\chi + \chi^2$$

Liquid Multiplier:

$$\phi_l = 1 + \frac{C}{\chi} + \frac{1}{\chi^2}$$

Where χ is the Lockhart-Martinelli Parameter and C is the Lockhart-Martinelli Constant. Both parameters can be solved for with the equations shown below:

Lockhart-Martinelli Parameter:

$$\chi = \sqrt{\frac{\Delta p_{frictional-liquid}}{\Delta p_{frictional-gas}}}$$

Lockhart-Martinelli Constant:

$$C = \begin{cases} 20 & Re_l > 1500, \quad Re_g > 1500 \\ 12 & Re_l < 1500, \quad Re_g > 1500 \\ 10 & Re_l > 1500, \quad Re_g < 1500 \\ 05 & Re_l < 1500, \quad Re_g < 1500 \end{cases}$$

A table below summarizes the important values in a two phase flow experiment:

Minimum Case				
Pressure Generation (Pa)	Momentum Pressure Loss (Pa)	Frictional Pressure Loss (Pa)	Total Pressure Loss (Pa)	Net Pressure (Pa)
42.5	0.0076	0.82	0.828	41.67

Maximum Case				
Pressure Generation (Pa)	Momentum Pressure Loss (Pa)	Frictional Pressure Loss (Pa)	Total Pressure Loss (Pa)	Net Pressure (Pa)
96.0	3.64	31.95	35.6	60.4

From the table above, it can be concluded that the pressure losses experienced in a two phase flow are much greater than those in single phase. Shown below is a graph depicting the net pressure as a function of the applied voltage in a two phase experiment:
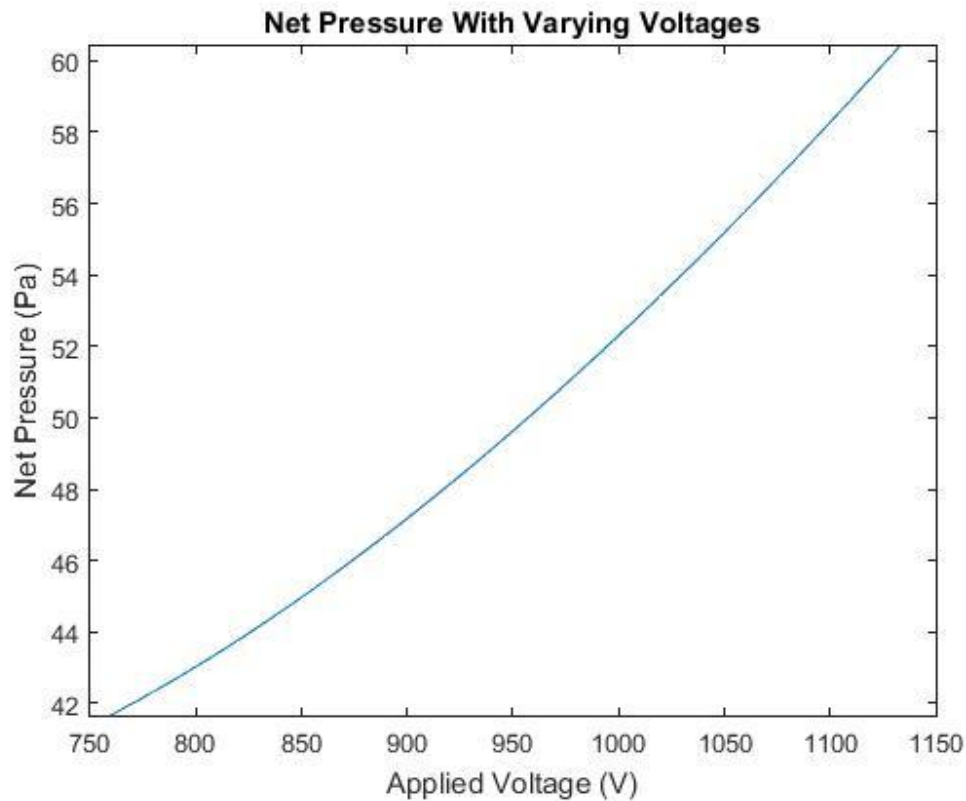
2.5 Evaporator Power Input Calculations

To initiate the phase change from the liquid phase to the vapor phase, the applied power to the evaporator must be calculated; the applied power will vary based on the working fluid. This calculation can be done by the equation shown below:

$$Q_{evaporator} = \dot{m}Lx$$

Where $\dot{m}$ is the mass flow rate, L is the latent heat of the working fluid at room temperature, and x is the vapor quality. The vapor quality is assumed to be 1 since a full phase change is desired in the evaporator. Based on this calculation for various flow rates, the maximum applied power to the evaporator is approximately 4.1 W.

2.6 Condenser Length Calculations

In order to change from the vapor phase to the liquid phase, it is important to calculate the length of a condenser. Now that the maximum power is accounted for, a maximum length can be calculated for the condenser, which initiates the condensation stage in the loop. The amount of energy required to evaporate a working fluid is the same as the amount of energy needed to condense a working fluid as shown below:

$$Q_{condenser} = Q_{evaporator}$$

To calculate the required length of the condenser, it is important to include all forms of heat transfer in the overall heat transfer equation. There are three instances where heat transfer is present: convection between the iced bath and the condenser, conduction in the metal pipe, and convection between the working fluid and the pipe walls. One assumption that can be made is that the iced bath is cold enough that the surface temperature throughout the entire condenser is at 273.15 K. As a result, the overall heat transfer equation is shown below:

$$Q_{condenser} = \frac{\pi D_i (T_c - T_b) L}{\frac{1}{h_i} + \frac{\ln\left(\frac{r_2}{r_1}\right) D_i}{2k}}$$

Where D_i is the inner diameter of the pipe, T_c is the subcool temperature of the working fluid (298.15 K), T_b is the overheated temperature of the working fluid (302.15 K), L is the length of the condenser, h_i is the average heat transfer coefficient of the working fluid, r_1 is the inner radius of the pipe, r_2 is the outer radius of the pipe, and k is the thermal conductivity of the pipe.

To avoid errors when calculating the heat transfer coefficient, the inlet of the pipe is considered to be at 99% vapor quality while the outlet of the pipe is at 1% vapor quality. Almost all variables in the heat transfer equation are known besides the length of the condenser and the heat transfer coefficient. Shown below is the equation used to solve for the heat transfer coefficient in a two phase flow:

$$h(x) = h_L \left((1-x)^{0.8} + \frac{3.8x^{0.76}(1-x)^{0.04}}{(p^+)^{0.38}} \right)$$

Where h_L is the liquid heat transfer coefficient, x is the vapor quality, and p^+ is the ratio between the saturated and critical pressures of the working fluid. The liquid heat transfer coefficient can be solved for by using the equation shown below:

$$h_L = 0.023 \left(\frac{GD_i}{\mu_f} \right)^{0.8} Pr_f^{0.4} \frac{k_f}{D_i}$$

Where G is the mass flow rate flux, D_i is the inner diameter of the pipe, μ_f is the dynamic viscosity of the working fluid as a saturated liquid, Pr_f is the Prandtl number of the working fluid as a saturated liquid, and k_f is the thermal conductivity of the working fluid as a saturated liquid. The Prandtl number can be calculated by using the equation:

$$Pr_f = \frac{c_p \mu_f}{k_f}$$

Where c_p is the specific heat at constant pressure and all other variables were previously mentioned in the liquid heat transfer coefficient equation. The average heat transfer coefficient can be calculated by averaging the heat transfer coefficient between the inlet and outlet of the condenser. At the highest flow rate of 1 mL/min, the yielded average heat transfer coefficient was 44.15 W/m^{2}K.

The remaining value that has not been calculated for is the condenser length. By

manipulating the heat transfer equation, the condenser length can be solved for:

$$L = \frac{(Q_{condenser})\left(\dfrac{1}{h_i} + \dfrac{ln\left(\frac{r_2}{r_1}\right)D_i}{2k}\right)}{\pi D_i(T_c - T_b)}$$

Based on this equation, the condenser length was calculated to be 0.168 m. However, to ensure

that the working fluid fully condenses, a safety factor of approximately 2 is set to increase the

condenser length to 0.336 m.

Chapter 3 – Experimental Setup

3.1 Preliminary Loop Design – 2D Sketch

The initial phase of this design was based off a previous experiment's test loop [5], but

with modifications. Shown below is a 2D sketch of the test loop:
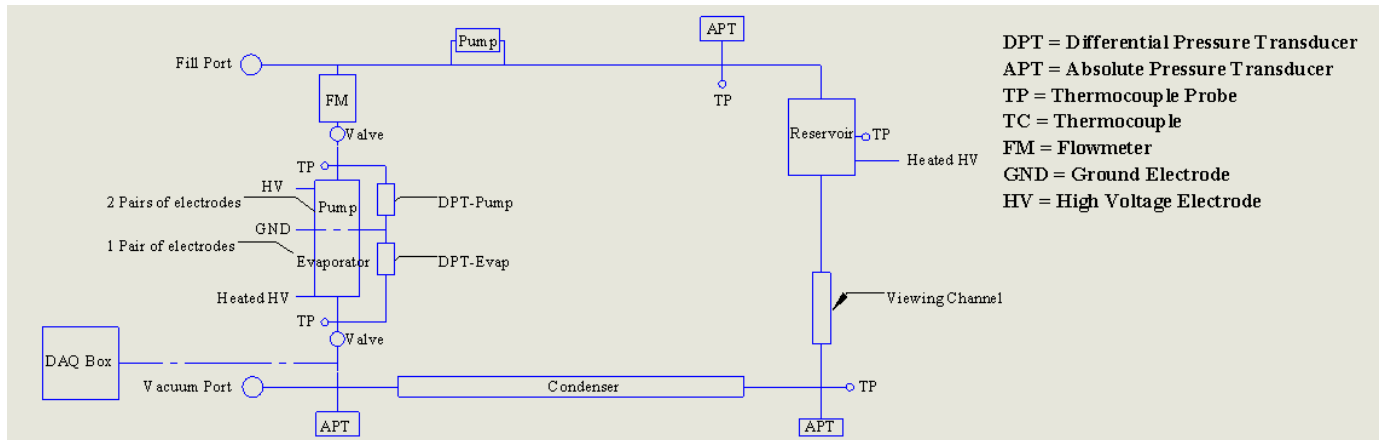
The reservoir tank provides a means of filling and extracting the working fluid. In addition, the

fill and vacuum ports provide the same function. An external pump is located upstream of the

pump and evaporator configuration to overcome large pressure losses that may arise during

experimentation. Both pump and evaporator are located in an integrated simple housing, each

with different high voltage sources for pressure generation. There is an additional wire

connection to power the heater for two phase experimentation. There is a condenser located downstream of the simple housing to initiate another phase change. A viewing channel is located at the end of the loop to ensure that the working fluid, after the condenser, is only in single phase.

There are three absolute pressure transducers (APTs) in experiment, each located at various sections of the loop exposed to drastic changes. One APT is located after the reservoir to ensure that the saturation pressure corresponds to the saturation temperature. Another APT is located after the evaporator exit to detect the pressure levels after a phase change. Since an additional phase change occurs in the condenser, an APT is conveniently located after the condenser exit. A flowmeter is located upstream of the integrated simple housing to monitor the flow rates entering that portion of the loop. Two differential pressure transducers (DPTs) are located at the heart of the experiment; one between the pump and another between the evaporator. These DPTs will provide experimental data for the amount of pressure generation taking place in each section of the integrated pumping system. Lastly, thermoprobes are widely used in the loop and strategically placed where a temperature change in the system may be present. In order to receive feedback from these sensors, all of their connections are made on one or more data acquisition boxes.

3.2 Loop Design – 3D Model

Based on the 2D sketch of the loop, a 3D model was created in SolidWorks to better understand how connections would come together. Shown below are the isometric and top views of the 3D model loop design:
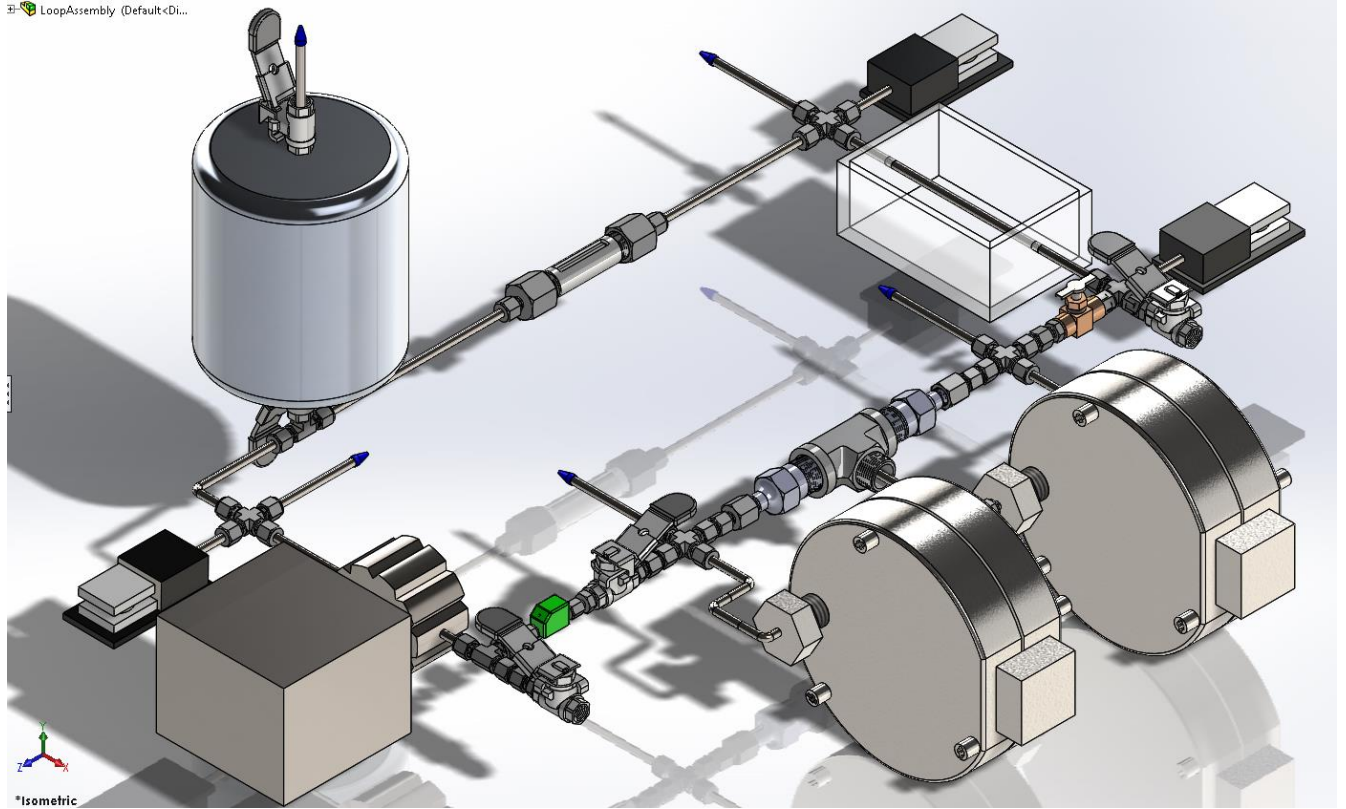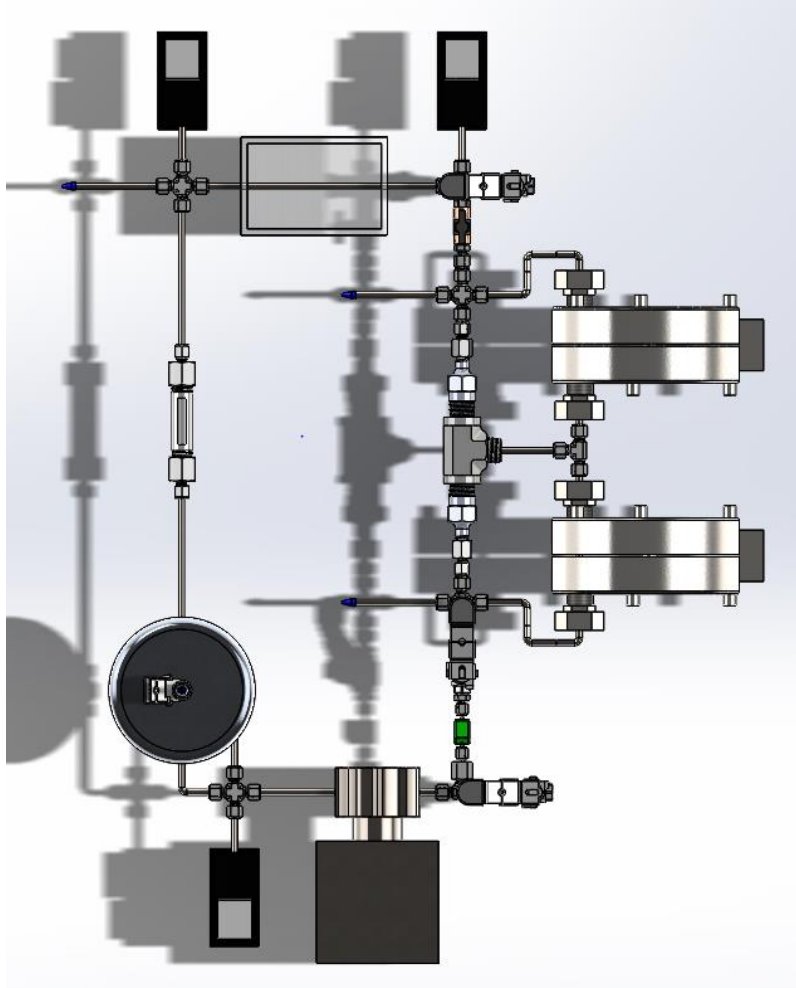
The majority of the tubes that exist in this assembly have an outer diameter of 6.35 mm in order stay relatively close to the intended micro-scale. Other sections of the loop are slightly larger in diameter to accommodate for the insertion of the simple housing. Stainless steel fittings are used to withstand the corroding effects of the working fluid. In addition, these steel fittings are Yor-Lok compression fittings that prevent large amounts of leaking. To further secure the simple housing in the large tee channel, o-rings are placed at each end. A visual representation of this is shown below:

Based on this configuration, the majority of the working fluid will be forced to flow axially. However, some of the fluid can flow out of the simple housing. As a solution, the fluid flowing outside of the simple housing will all flow to a junction shared by both differential pressure transducers. Due to the time constraints, the MQP assembly was not fully completed. Therefore, there is no experimental data. Shown below are different views of the current assembly:
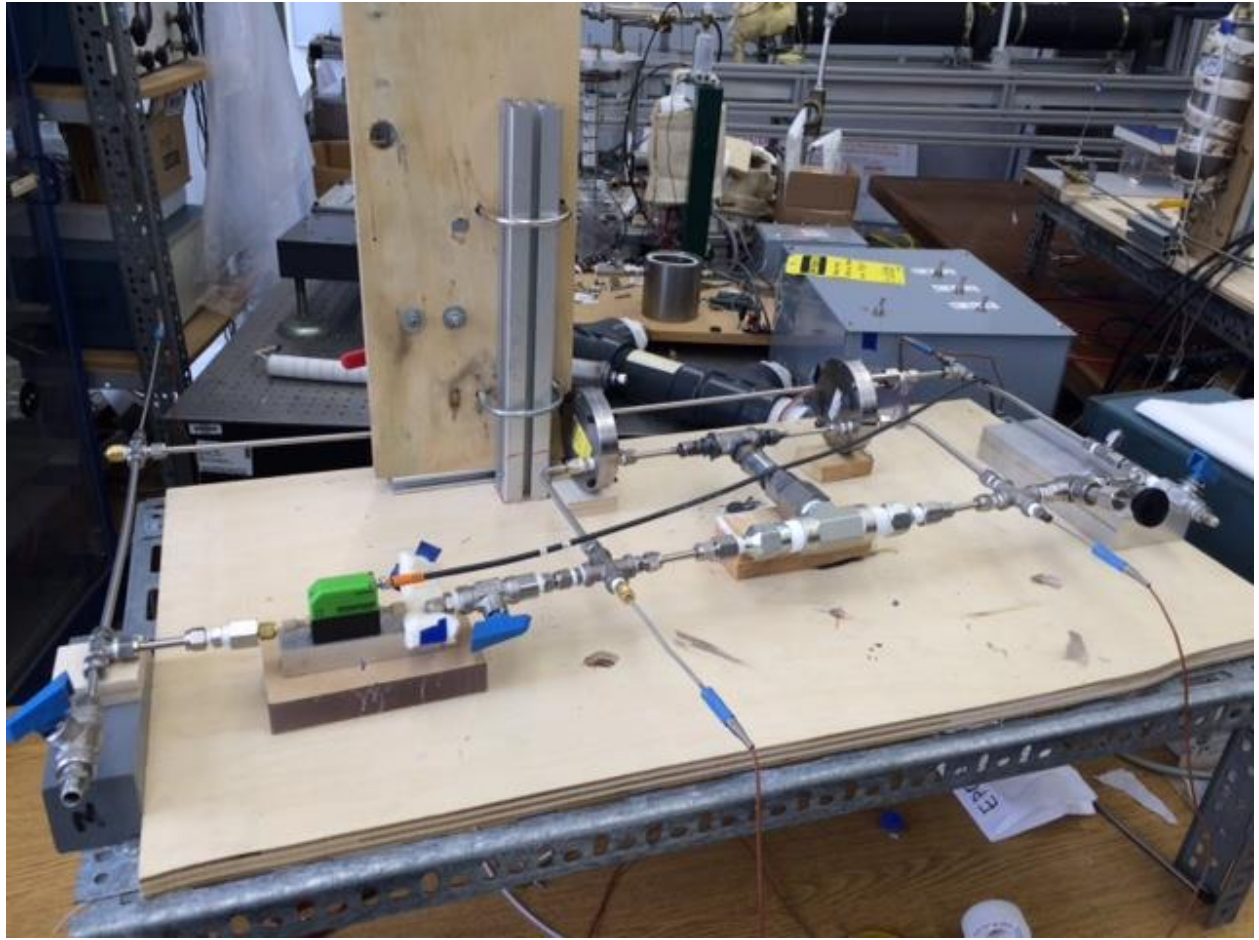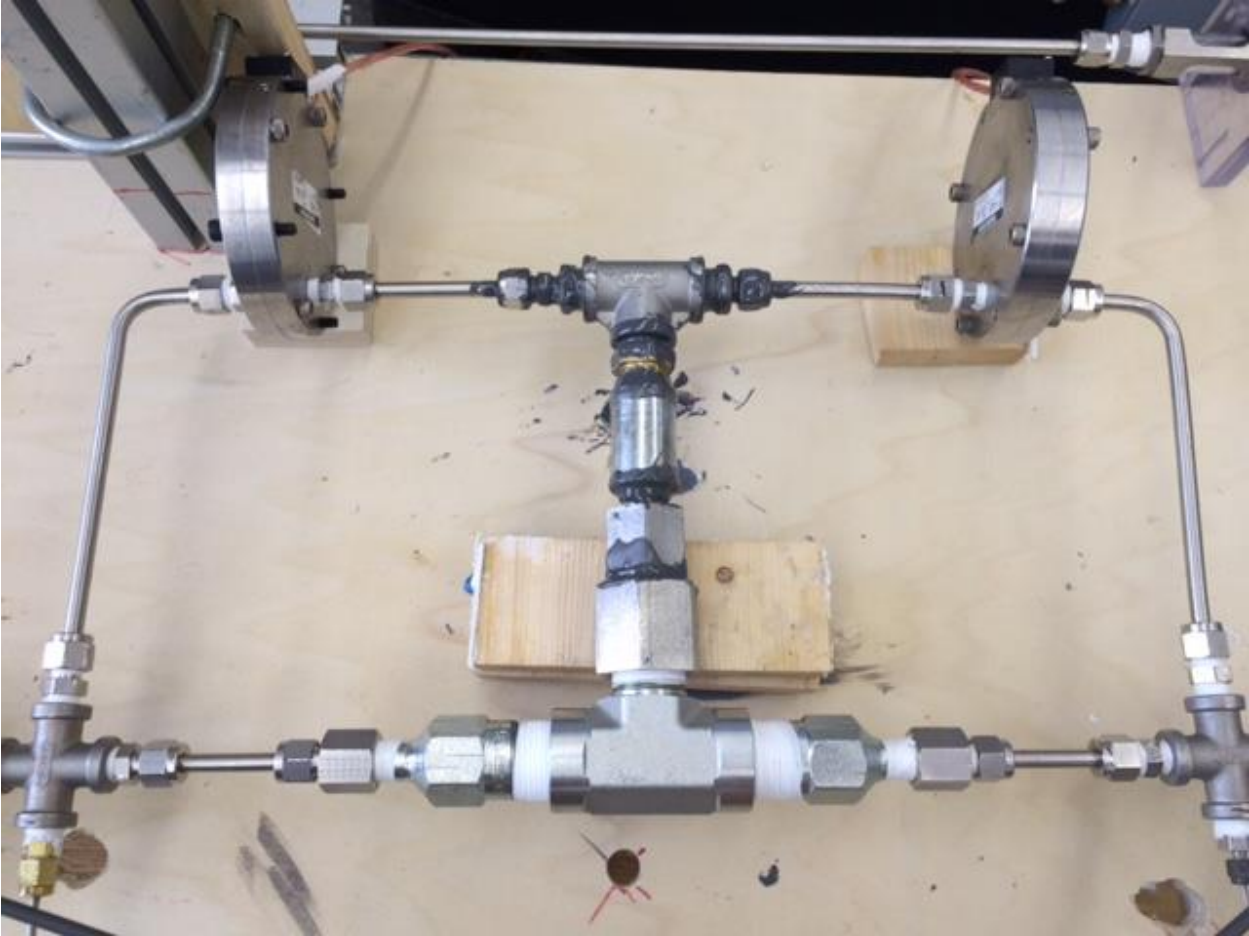
References

1. "Understanding of electrohydrodynamic conduction pumping phenomenon" - Yinshan Feng and Jamal Seyed-Yagoobi

2. "Electrohydrodynamic pumping of dielectric liquids" - Jamal Seyed-Yagoobi

3. "Dielectric Fluid Flow Generation in Meso-tubes with Micro-scale Electrohydrodynamic Conduction Pumping" - Viral K. Patel and Jamal Seyed-Yagoobi

4. "Flow Generation and distribution control in Meso Scale via Electrohydrodynamic Conduction Pumping" – MQP 2015

5. "Electrohydrodynamic Pumping Pressure Generation" – MQP 2013

6. http://wwwme.nchu.edu.tw/Enter/html/lab/lab516/Heat%20Transfer/chapter_3.pdf (Yoav Peles, Department of Mechanical, Aerospace and Nuclear Engineering Rensselaer Polytechnic Institute)

7. "Development of EHD Ion-Drag Micropump for Microscale Electronics Cooling" – A.J. Robinson

8. "Terrestrial and Micro-gravity Experimental Study of Micro-scale Heat Transport Device Driven by Electrohydrodynamic Conduction Pumping" – Franklin Robinson and Viral K. Patel

9. IEEE Micro Electro Mechanical Systems NMMS-90 Conference, Napa Valley, CA, U.S.A., Feb. 19-21, 1990

10. "Electrohydrodynamic Induction Pumping of Liquid Film in Vertical Annular Configuration" - S. A. Aldini and J. Seyed-Yagoobi

11. "Augmentation of Two-Phase and Single-Phase Heat Transfer and Mass Transport with Electrohydrodynamics in Thermal Equipment"- J. Seyed-Yagoobi, 1999

12. "Advances in Electrohydrodynamic Conduction Pumping" - Pearson and J. Seyed-Yagoobi 2008

13. "Electrical forces in the bulk: Injection, Conduction and Induction EHD micropumps" - http://laplace.us.es/cism09/EHD_Micropumps_Section2.pdf

Appendices

Appendix A – MATLAB Scripts

Single Phase Pressure Generation and Pressure Loss:

```
%---Code written by: Darien Nate Khea, Date written on: 11/01/2015---%

%---Pressure Generation Calculation (Feng Paper)---%

V_pump = [750:10:1240]; %Voltage range applied at pump section [V]

d_electrode = 0.001; %Distance between electrodes [m]

epsilon_R123 = 42.8*10^-12; %Permittivity of R123 [Farads/m]

m_p = 2; %Number of electrode pairs in Pump Section

m_e = 1; %Number of electrode pairs in Evaporator Section

P_pump_generation =
(0.6875*0.85)*m_p*epsilon_R123.*((V_pump.^2)./(d_electrode^2)); %Pressure
generation from pump [Pa]

P_evaporator_generation =
(0.6875*0.85)*m_e*epsilon_R123.*((V_pump.^2)./(d_electrode^2)); %Pressure
generation from evaporator [Pa]

plot(V_pump,P_pump_generation, V_pump, P_evaporator_generation); %plots graph

xlim([750 1240]); %limits axis

xlabel('Applied Voltage (V)'); %labels x-axis

ylabel('Pressure Generation (Pa)'); %labels y-axis

title('Theoretical Pressure Generation With Varying Voltages'); %labels title

legend('Pump','Evaporator'); %labels legend

%---Pressure Loss Calculation (Purely Darcy-Weisbach Equation)---%

l_pump = 39.58*10^-3; %Length of pump[m]

l_evaporator = 11.46*10^-3; %Length of evaporator [m]

l_channel = 3; %Length of remaining channel (condenser included) [m] -Max
Value-

D_pump = 1.61*10^-3; %Diameter of pump [m]
```

```matlab
D_evaporator = 1.61*10^-3; %Diameter of evaporator [m]

D_channel = 4.57*10^-3; %Diameter of remaining channel (condenser included)
[m] - 0.18 inch.

rho_R123 = 1458.8; %Density of R123 [kg/m^3]

mu_R123 = 4.0805*10^-4; %Dynamic viscosity of R123 [kg/(m*s)]

a_pump = (pi*D_pump^2)/4; %Area of pump [m^2]

a_evaporator = (pi*D_evaporator^2)/4; %Area of evaporator [m^2]

a_channel = (pi*D_channel^2)/4; %Area of remaining channel (condenser
included) [m^2]

m_dot = [2.43*10^-6:2.43*10^-6:1.22*10^-4]; %Desired mass flowrate range
[kg/s] (0.1 mL/min:0.1 mL/min:5 mL/min)

vel_pump = m_dot./(rho_R123*a_pump); %Velocity range in pump [m/s]

vel_evaporator = m_dot./(rho_R123*a_evaporator); %Velocity range in
evaporator[m/s]

vel_channel = m_dot./(rho_R123*a_channel); %Velocity range in remaining
channel (condenser included) [m/s]

Re_pump = (rho_R123*D_pump.*vel_pump)./mu_R123; %Reynolds number of fluid in
pump [dimensionless]

Re_evaporator = (rho_R123*D_evaporator.*vel_evaporator)./mu_R123; %Reynolds
number of fluid in evaporator [dimensionless]

Re_channel = (rho_R123*D_channel.*vel_channel)./mu_R123; %Reynolds number of
fluid in channel [dimensionless]

f_pump = 64./Re_pump; %Friction factor of pump [dimensionless]

f_evaporator = 64./Re_evaporator; %Friction factor of evaporator
[dimensionless]

f_channel = 64./Re_channel; %Friction factor of channel [dimensionless]

P_loss_pump = (f_pump.*l_pump.*rho_R123.*(vel_pump.^2))./(D_pump*2);
%Pressure Loss in Pump [Pa]

P_loss_evaporator =
(f_evaporator.*l_evaporator.*rho_R123.*(vel_evaporator.^2))./(D_pump*2);
%Pressure Loss in Evaporator [Pa]
```

```matlab
P_loss_channel =
(f_channel.*l_channel.*rho_R123.*(vel_channel.^2))./(D_channel*2); %Pressure
Loss in Channel (condenser included) [Pa] -Over Estimating-

Total_Pressure_Loss = P_loss_pump+P_loss_evaporator+P_loss_channel; %Total
Pressure Loss in Loop [Pa]

%---Net Pressure Calculation---%

Net_Pressure = P_pump_generation+P_evaporator_generation-Total_Pressure_Loss;
%Net pressure in loop [Pa]

plot(V_pump, Net_Pressure); %plots graph

xlim([750 1240]); %limits axis

xlabel('Applied Voltage (V)'); %labels x-axis

ylabel('Net Pressure (Pa)'); %labels y-axis

title('Net Pressure With Varying Voltages'); %labels title
```

__Two Phase Pressure Loss:__

```matlab
%---Code written by: Darien Nate Khea, Date written on: 11/01/2015---%

%---Pressure Generation Calculation (Feng Paper)---%

V_pump = [750:10:1240]; %Voltage range applied at pump + evaporator section
[V]

d_electrode = 0.001; %Distance between electrodes [m]

epsilon_R123 = 42.8*10^-12; %Permittivity of R123 [Farads/m]

m = 3; %Number of electrode pairs in pump + evaporator section

P_pump_generation =
(0.6875*0.85)*m*epsilon_R123.*((V_pump.^2)./(d_electrode^2)); %Pressure
generation from pump + evaporator [Pa]

%---Pressure Loss Calculation in Single Phase Sections (Darcy-Weisbach
Equation)---%

l_pump = 39.58*10^-3; %Length of pump[m]

l_channel_single = 1.5; %Length of channel with single phase flow [m] -Max
Value-

D_pump = 1.61*10^-3; %Diameter of pump [m]
```

```matlab
D_channel_single = 5.08*10^-3; %Diameter of channel with single phase flow
[m] - 1/5 inch.

rho_R123 = 1458.8; %Density of R123 [kg/m^3]

mu_R123 = 4.0805*10^-4; %Dynamic viscosity of R123 [kg/(m*s)]

a_pump = (pi*D_pump^2)/4; %Area of pump [m^2]

a_channel_single = (pi*D_channel_single^2)/4; %Area of channel with single
phase flow [m^2]

m_dot = [2.43*10^-6:2.43*10^-6:1.22*10^-4]; %Desired mass flowrate range
[kg/s] (0.1 mL/min:0.1 mL/min:5 mL/min)

vel_pump = m_dot./(rho_R123*a_pump); %Velocity range in pump [m/s]

vel_channel_single = m_dot./(rho_R123*a_channel_single); %Velocity range in
channel with single phase flow [m/s]

Re_pump = (rho_R123*D_pump.*vel_pump)./mu_R123; %Reynolds number of fluid in
pump [dimensionless]

Re_channel_single = (rho_R123*D_channel_single.*vel_channel_single)./mu_R123;
%Reynolds number of fluid in single phase flow in channel [dimensionless]

f_pump = 64./Re_pump; %Friction factor of pump [dimensionless]

f_channel_single = 64./Re_channel_single; %Friction factor of channel with
single phase flow [dimensionless]

P_loss_pump = (f_pump.*l_pump.*rho_R123.*(vel_pump.^2))./(D_pump*2);
%Pressure Loss in Pump [Pa]

P_loss_channel_single =
(f_channel_single.*l_channel_single.*rho_R123.*(vel_channel_single.^2))./(D_c
hannel_single*2); %Pressure Loss in Channel with single phase flow [Pa] -Over
Estimating-

Total_Pressure_Loss_single = P_loss_pump+P_loss_channel_single; %Total
Pressure Loss in single phase flow sections in loop [Pa]

%---Pressure Loss Calculation in Two Phase Sections (Lockhart-Martinelli
Equation)---%

%---Initial Parameters---%

l_evaporator = 11.46*10^-3; %Length of evaporator [m]

l_condenser = 0.3; %Length of condenser [m]

l_channel_two = 0.2; %Length of channel with two phase flow [m] -Max Value-
```

```matlab
D_evaporator = 1.61*10^-3; %Diameter of evaporator [m]

D_condenser = 6.35*10^-3; %Diameter of condenser [m] - 1/4 inch.

D_channel_two = 5.08*10^-3; %Diameter of channel with two phase flow [m] -
1/5 inch.

a_evaporator = (pi*D_evaporator^2)/4; %Area of evaporator [m^2]

a_condenser = (pi*D_condenser^2)/4; %Area of condenser [m^2]

a_channel_two = (pi*D_channel_two^2)/4; %Area of channel with two phase flow
[m^2]

g = 9.81; %Acceleration due to gravity [m/s^2]

%---Momentun Pressure Loss---%

%---Mass Flowrate Flux---%

G_evaporator = m_dot./a_evaporator; %Mass flowrate flux in evaporator [kg/(s-
m^2)]

G_condenser = m_dot./a_condenser; %Mass flowrate flux in condenser [kg/(s-
m^2)]

G_channel_two = m_dot./a_channel_two; %Mass flowrate flux in channel with two
phase [kg/(s-m^2)]

%---Vapor Quality---%

x_evaporator_i = 0.001; %Vapor quality in evaporator inlet [dimensionless]

x_evaporator_o = 0.05; %Vapor quality in evaporator outlet [dimensionless]

x_condenser_i = 0.001; %Vapor quality in condenser inlet [dimensionless]

x_condenser_o = 0.05; %Vapor quality in condenser outlet [dimensionless]

x_channel_two_i = 0.05; %Vapor quality in channel with two phase flow inlet
[dimensionless]

x_channel_two_o = 0.05; %Vapor quality in channel with two phase flow outlet
[dimensionless]

%---Density of R123 for Saturated Liquid---%

rho_R123_liquid_evaporator = 1457; %Density for liquid phase in evaporator
[kg/m^3] -Midpoint between high and low temperatures-

rho_R123_liquid_condenser = 1467; %Density for liquid phase in condenser
[kg/m^3] -Midpoint between high and low temperatures-
```

```matlab
rho_R123_liquid_channel_two = 1457; %Density for liquid phase in channel
[kg/m^3] -Midpoint between high and low temperatures-

%---Density of R123 for Saturated Vapor---%

rho_R123_vapor_evaporator = 6.5; %Density for vapor phase in evaporator
[kg/m^3] -Midpoint between high and low temperatures-

rho_R123_vapor_condenser = 5.75; %Density for vapor phase in condenser
[kg/m^3] -Midpoint between high and low temperatures-

rho_R123_vapor_channel_two = 6.5; %Density for vapor phase in channel
[kg/m^3] -Midpoint between high and low temperatures-

%---Surface Tension of R123---%

sigma_evaporator = 0.015; %Surface tension of R123 in evaporator [N/m]

sigma_condenser = 0.015; %Surface tension of R123 in condenser [N/m]

sigma_channel_two= 0.016; %Surface tension of R123 in channel with two phase
[N/m]

%---Void Fraction---%

epsilon_evaporator_i =
(x_evaporator_i/rho_R123_vapor_evaporator)*(((1+0.12*(1-
x_evaporator_i))*((x_evaporator_i/rho_R123_vapor_evaporator)+((1-
x_evaporator_i)/rho_R123_liquid_evaporator)))+((1.18*(1-
x_evaporator_i)*(g*sigma_evaporator*(rho_R123_liquid_evaporator-
rho_R123_vapor_evaporator))^0.25)./(G_evaporator.*(rho_R123_liquid_evaporator
)^0.5))).^-1; %Void fraction in evaporator inlet [dimensionless]

epsilon_evaporator_o =
(x_evaporator_o/rho_R123_vapor_evaporator)*(((1+0.12*(1-
x_evaporator_o))*((x_evaporator_o/rho_R123_vapor_evaporator)+((1-
x_evaporator_o)/rho_R123_liquid_evaporator)))+((1.18*(1-
x_evaporator_o)*(g*sigma_evaporator*(rho_R123_liquid_evaporator-
rho_R123_vapor_evaporator))^0.25)./(G_evaporator.*(rho_R123_liquid_evaporator
)^0.5))).^-1; %Void fraction in evaporator outlet [dimensionless]

epsilon_condenser_i = (x_condenser_i/rho_R123_vapor_condenser)*(((1+0.12*(1-
x_condenser_i))*((x_condenser_i/rho_R123_vapor_condenser)+((1-
x_condenser_i)/rho_R123_liquid_condenser)))+((1.18*(1-
x_condenser_i)*(g*sigma_condenser*(rho_R123_liquid_condenser-
rho_R123_vapor_condenser))^0.25)./(G_condenser.*(rho_R123_liquid_condenser)^0
.5))).^-1; %Void fraction in condenser inlet [dimensionless]

epsilon_condenser_o = (x_condenser_o/rho_R123_vapor_condenser)*(((1+0.12*(1-
x_condenser_o))*((x_condenser_o/rho_R123_vapor_condenser)+((1-
x_condenser_o)/rho_R123_liquid_condenser)))+((1.18*(1-
x_condenser_o)*(g*sigma_condenser*(rho_R123_liquid_condenser-
```

```matlab
rho_R123_vapor_condenser))^0.25)./(G_condenser.*(rho_R123_liquid_condenser)^0
.5))).^-1; %Void fraction in condenser outlet [dimensionless]

epsilon_channel_two_i =
(x_channel_two_i/rho_R123_vapor_channel_two)*(((1+0.12*(1-
x_channel_two_i))*((x_channel_two_i/rho_R123_vapor_channel_two)+((1-
x_channel_two_i)/rho_R123_liquid_channel_two)))+((1.18*(1-
x_channel_two_i)*(g*sigma_channel_two*(rho_R123_liquid_channel_two-
rho_R123_vapor_channel_two))^0.25)./(G_channel_two.*(rho_R123_liquid_channel_
two)^0.5))).^-1; %Void fraction in channel with two phase inlet
[dimensionless]

epsilon_channel_two_o =
(x_channel_two_o/rho_R123_vapor_channel_two)*(((1+0.12*(1-
x_channel_two_o))*((x_channel_two_o/rho_R123_vapor_channel_two)+((1-
x_channel_two_o)/rho_R123_liquid_channel_two)))+((1.18*(1-
x_channel_two_o)*(g*sigma_channel_two*(rho_R123_liquid_channel_two-
rho_R123_vapor_channel_two))^0.25)./(G_channel_two.*(rho_R123_liquid_channel_
two)^0.5))).^-1; %Void fraction in channel with two phase outlet
[dimensionless]

%---Momentum Pressure Loss Calculation---%

M_pressure_loss_evaporator = G_evaporator.^2.*((((1-
x_evaporator_o)^2./(rho_R123_liquid_evaporator*(1-
epsilon_evaporator_o)))+(x_evaporator_o^2./(rho_R123_vapor_evaporator*epsilon
_evaporator_o)))-(((1-x_evaporator_i)^2./(rho_R123_liquid_evaporator*(1-
epsilon_evaporator_i)))+(x_evaporator_i^2./(rho_R123_vapor_evaporator*epsilon
_evaporator_i)))); %Momentum pressure loss in evaporator [Pa]

M_pressure_loss_condenser = G_condenser.^2.*((((1-
x_condenser_o)^2./(rho_R123_liquid_condenser*(1-
epsilon_condenser_o)))+(x_condenser_o^2./(rho_R123_vapor_condenser*epsilon_co
ndenser_o)))-(((1-x_condenser_i)^2./(rho_R123_liquid_condenser*(1-
epsilon_condenser_i)))+(x_condenser_i^2./(rho_R123_vapor_condenser*epsilon_co
ndenser_i)))); %Momentum pressure loss in condenser [Pa]

M_pressure_loss_channel_two = G_channel_two.^2.*((((1-
x_channel_two_o)^2./(rho_R123_liquid_channel_two*(1-
epsilon_channel_two_o)))+(x_channel_two_o^2./(rho_R123_vapor_channel_two*epsi
lon_channel_two_o)))-(((1-
x_channel_two_i)^2./(rho_R123_liquid_channel_two*(1-
epsilon_channel_two_i)))+(x_channel_two_i^2./(rho_R123_vapor_channel_two*epsi
lon_channel_two_i)))); %Momentum pressure loss in channel with two phase [Pa]

%---Frictional Pressure Loss---%

%---Reynolds Number---%

%---Viscosity of R123 liquid---%

mu_liquid_R123_e = 4*10^-4; %Viscosity of saturated liquid in evaporator [Pa-
s] -Approximation-
```

```matlab
mu_liquid_R123_con = 4.25*10^-4; %Viscosity of saturated liquid in condenser
[Pa-s] -Approximation-

mu_liquid_R123_ch = 4*10^-4; %Viscosity of saturated liquid in channel with
two phase flow [Pa-s] -Approximation-

%---Viscosity of R123 gas---%

mu_vapor_R123_e = 1.1*10^-5; %Viscosity of saturated vapor in evaporator [Pa-
s] -Approximation-

mu_vapor_R123_con = 1.07*10^-5; %Viscosity of saturated vapor in condenser
[Pa-s] -Approximation-

mu_vapor_R123_ch = 1.1*10^-5; %Viscosity of saturated vapor in channel with
two phase flow [Pa-s] -Approximation-

%---Reynolds Number for Saturated Liquid---%

Re_liquid_evaporator_i = (G_evaporator.*(1-
x_evaporator_i)*D_evaporator)./(mu_liquid_R123_e) ; %Reynolds number of
liquid phase for evaporator entrance [dimensionless]

Re_liquid_evaporator_o = (G_evaporator.*(1-
x_evaporator_o)*D_evaporator)./(mu_liquid_R123_e); %Reynolds number of liquid
phase for evaporator exit [dimensionless]

Re_liquid_condenser_i = (G_condenser.*(1-
x_condenser_i)*D_condenser)./(mu_liquid_R123_con); %Reynolds number of liquid
phase for condenser entrance [dimensionless]

Re_liquid_condenser_o = (G_condenser.*(1-
x_condenser_o)*D_condenser)./(mu_liquid_R123_con); %Reynolds number of liquid
phase for condenser exit [dimensionless]

Re_liquid_channel_two_i = (G_channel_two.*(1-
x_channel_two_i)*D_channel_two)./(mu_liquid_R123_ch); %Reynolds number of
liquid phase for channel entrance [dimensionless]

Re_liquid_channel_two_o = (G_channel_two.*(1-
x_channel_two_o)*D_channel_two)./(mu_liquid_R123_ch); %Reynolds number of
liquidp hase for channel exit [dimensionless]

%---Reynolds Number for Satured Vapor---%

Re_vapor_evaporator_i =
(G_evaporator.*(x_evaporator_i)*D_evaporator)./(mu_vapor_R123_e) ; %Reynolds
number vapor phase for evaporator entrance [dimensionless]

Re_vapor_evaporator_o =
(G_evaporator.*(x_evaporator_o)*D_evaporator)./(mu_vapor_R123_e); %Reynolds
number vapor phase for evaporator exit [dimensionless]
```

```matlab
Re_vapor_condenser_i = ...
(G_condenser.*(x_condenser_i)*D_condenser)./(mu_vapor_R123_con); %Reynolds
number vapor phase for condenser entrance [dimensionless]

Re_vapor_condenser_o = ...
(G_condenser.*(x_condenser_o)*D_condenser)./(mu_vapor_R123_con); %Reynolds
number vapor phase for for condenser exit [dimensionless]

Re_vapor_channel_two_i = ...
(G_channel_two.*(x_channel_two_i)*D_channel_two)./(mu_vapor_R123_ch);
%Reynolds number vapor phase for channel entrance [dimensionless]

Re_vapor_channel_two_o = ...
(G_channel_two.*(x_channel_two_o)*D_channel_two)./(mu_vapor_R123_ch);
%Reynolds number vapor phase for channel exit [dimensionless]

%---Friction Factor (Conditional for 10% Vapor) For Saturated Liquid---%

f_liquid_evaporator_i = 16./Re_liquid_evaporator_i; %Friction factor for
liquid phase for evaporator entrance [dimensionless]

f_liquid_evaporator_o = 16./Re_liquid_evaporator_o; %Friction factor for
liquid phase for evaporator exit [dimensionless]

f_liquid_condenser_i = 16./Re_liquid_condenser_i; %Friction factor for liquid
phase for condenser entrance [dimensionless]

f_liquid_condenser_o = 16./Re_liquid_condenser_o; %Friction factor for liquid
phase for condenser exit [dimensionless]

f_liquid_channel_two_i = 16./Re_liquid_channel_two_i; %Friction factor for
liquid phase for channel entrance [dimensionless]

f_liquid_channel_two_o = 16./Re_liquid_channel_two_o; %Friction factor for
liquid phase for channel exit [dimensionless]

%---Friction Factor (Conditional for 10% Vapor) For Saturated Vapor---%

f_vapor_evaporator_i = 16./Re_vapor_evaporator_i; %Friction factor for vapor
phase for evaporator entrance [dimensionless]

f_vapor_evaporator_o = 16./Re_vapor_evaporator_o; %Friction factor for vapor
phase for evaporator exit [dimensionless]

f_vapor_condenser_i = 16./Re_vapor_condenser_i; %Friction factor for vapor
phase for condenser entrance [dimensionless]

f_vapor_condenser_o = 16./Re_vapor_condenser_o; %Friction factor for vapor
phase for condenser exit [dimensionless]

f_vapor_channel_two_i = 16./Re_vapor_channel_two_i; %Friction factor for
vapor phase for channel entrance [dimensionless]
```

```matlab
f_vapor_channel_two_o = 16./Re_vapor_channel_two_o; %Friction factor for
vapor phase for channel exit [dimensionless]

%---Frictional Pressure Loss - Intermediate For Saturated Liquid---%

f_loss_liquid_evaporator_i =
(4*f_liquid_evaporator_i.*l_evaporator.*G_evaporator.^2.*(1-
x_evaporator_i)^2)/(2*rho_R123_liquid_evaporator*D_evaporator);

f_loss_liquid_evaporator_o =
(4*f_liquid_evaporator_o.*l_evaporator.*G_evaporator.^2.*(1-
x_evaporator_o)^2)/(2*rho_R123_liquid_evaporator*D_evaporator);

f_loss_liquid_condenser_i =
(4*f_liquid_condenser_i.*l_condenser.*G_condenser.^2.*(1-
x_condenser_i)^2)/(2*rho_R123_liquid_condenser*D_condenser);

f_loss_liquid_condenser_o =
(4*f_liquid_condenser_o.*l_condenser.*G_condenser.^2.*(1-
x_condenser_o)^2)/(2*rho_R123_liquid_condenser*D_condenser);

f_loss_liquid_channel_two_i =
(4*f_liquid_channel_two_i.*l_channel_two.*G_channel_two.^2.*(1-
x_channel_two_i)^2)/(2*rho_R123_liquid_channel_two*D_channel_two);

f_loss_liquid_channel_two_o =
(4*f_liquid_channel_two_o.*l_channel_two.*G_channel_two.^2.*(1-
x_channel_two_o)^2)/(2*rho_R123_liquid_channel_two*D_channel_two);

%---Frictional Pressure Loss - Intermediate For Saturated Vapor---%

f_loss_vapor_evaporator_i =
(4*f_vapor_evaporator_i.*l_evaporator.*G_evaporator.^2.*(x_evaporator_i)^2)/(
2*rho_R123_vapor_evaporator*D_evaporator);

f_loss_vapor_evaporator_o =
(4*f_vapor_evaporator_o.*l_evaporator.*G_evaporator.^2.*(x_evaporator_o)^2)/(
2*rho_R123_vapor_evaporator*D_evaporator);

f_loss_vapor_condenser_i =
(4*f_vapor_condenser_i.*l_condenser.*G_condenser.^2.*(x_condenser_i)^2)/(2*rh
o_R123_vapor_condenser*D_condenser);

f_loss_vapor_condenser_o =
(4*f_vapor_condenser_o.*l_condenser.*G_condenser.^2.*(x_condenser_o)^2)/(2*rh
o_R123_vapor_condenser*D_condenser);

f_loss_vapor_channel_two_i =
(4*f_vapor_channel_two_i.*l_channel_two.*G_channel_two.^2.*(x_channel_two_i)^
2)/(2*rho_R123_vapor_channel_two*D_channel_two);

f_loss_vapor_channel_two_o =
(4*f_vapor_channel_two_o.*l_channel_two.*G_channel_two.^2.*(x_channel_two_o)^
2)/(2*rho_R123_vapor_channel_two*D_channel_two);
```

```matlab
%---Lockhart-Martinelli Parameter---%

X_evaporator_i = sqrt(f_loss_liquid_evaporator_i./f_loss_vapor_evaporator_i);

X_condenser_i = sqrt(f_loss_liquid_evaporator_o./f_loss_vapor_evaporator_o);

X_channel_two_i = sqrt(f_loss_liquid_condenser_i./f_loss_vapor_condenser_i);

X_evaporator_o = sqrt(f_loss_liquid_condenser_o./f_loss_vapor_condenser_o);

X_condenser_o =
sqrt(f_loss_liquid_channel_two_i./f_loss_vapor_channel_two_i);

X_channel_two_o =
sqrt(f_loss_liquid_channel_two_o./f_loss_vapor_channel_two_o);

%---Lockhart-Martinelli Constant---%

%Since both liquid and vapor Reynolds numbers are less than 1500%

C = 5;

%---Liquid Multiplier---%

phi_liquid_evaporator_i = 1+(C./X_evaporator_i)+(1./X_evaporator_i.^2);

phi_liquid_evaporator_o = 1+(C./X_evaporator_o)+(1./X_evaporator_o.^2);

phi_liquid_condenser_i = 1+(C./X_condenser_i)+(1./X_condenser_i.^2);

phi_liquid_condenser_o = 1+(C./X_condenser_o)+(1./X_condenser_o.^2);

phi_liquid_channel_two_i = 1+(C./X_channel_two_i)+(1./X_channel_two_i.^2);

phi_liquid_channel_two_o = 1+(C./X_channel_two_o)+(1./X_channel_two_o.^2);

%---Gas Multiplier---%

phi_vapor_evaporator_i = 1+(C.*X_evaporator_i)+X_evaporator_i.^2;

phi_vapor_evaporator_o = 1+(C.*X_evaporator_o)+X_evaporator_o.^2;

phi_vapor_condenser_i = 1+(C.*X_condenser_i)+X_condenser_i.^2;

phi_vapor_condenser_o = 1+(C.*X_condenser_o)+X_condenser_o.^2;

phi_vapor_channel_two_i = 1+(C.*X_channel_two_i)+X_channel_two_i.^2;

phi_vapor_channel_two_o = 1+(C.*X_channel_two_o)+X_channel_two_o.^2;

%---Frictional Pressure Loss Liquid---%
```

```matlab
F_loss_liquid_evaporator_i =
(f_loss_liquid_evaporator_i.*phi_liquid_evaporator_i);

F_loss_liquid_evaporator_o =
(f_loss_liquid_evaporator_o.*phi_liquid_evaporator_o);

F_loss_liquid_condenser_i =
(f_loss_liquid_condenser_i.*phi_liquid_condenser_i);

F_loss_liquid_condenser_o =
(f_loss_liquid_condenser_o.*phi_liquid_condenser_o);

F_loss_liquid_channel_two_i =
(f_loss_liquid_channel_two_i.*phi_liquid_channel_two_i);

F_loss_liquid_channel_two_o =
(f_loss_liquid_channel_two_o.*phi_liquid_channel_two_o);

%---Frictional Pressure Loss Vapor---%

F_loss_vapor_evaporator_i =
(f_loss_vapor_evaporator_i.*phi_vapor_evaporator_i);

F_loss_vapor_evaporator_o =
(f_loss_vapor_evaporator_o.*phi_vapor_evaporator_o);

F_loss_vapor_condenser_i = (f_loss_vapor_condenser_i.*phi_vapor_condenser_i);

F_loss_vapor_condenser_o = (f_loss_vapor_condenser_o.*phi_vapor_condenser_o);

F_loss_vapor_channel_two_i =
(f_loss_vapor_channel_two_i.*phi_vapor_channel_two_i);

F_loss_vapor_channel_two_o =
(f_loss_vapor_channel_two_o.*phi_vapor_channel_two_o);

%---Frictional Pressure Loss Actual Liquid---%

F_loss_liquid_evaporator =
(F_loss_liquid_evaporator_i+F_loss_liquid_evaporator_o)/2;

F_loss_liquid_condenser =
(F_loss_liquid_condenser_i+F_loss_liquid_condenser_o)/2;

F_loss_liquid_channel_two =
(F_loss_liquid_channel_two_i+F_loss_liquid_channel_two_o)/2;

%---Frictional Pressure Loss Actual Vapor---%

F_loss_vapor_evaporator =
(F_loss_vapor_evaporator_i+F_loss_vapor_evaporator_o)/2;
```

```
F_loss_vapor_condenser =
(F_loss_vapor_condenser_i+F_loss_vapor_condenser_o)/2;

F_loss_vapor_channel_two =
(F_loss_vapor_channel_two_i+F_loss_vapor_channel_two_o)/2;

%---Two Phase Total Pressure Loss---%

Total_Pressure_Loss_two =
F_loss_liquid_evaporator+F_loss_liquid_condenser+F_loss_liquid_channel_two+F_
loss_vapor_evaporator+F_loss_vapor_condenser+F_loss_vapor_channel_two+M_press
ure_loss_evaporator+M_pressure_loss_condenser+M_pressure_loss_channel_two;

%---Total Pressure Loss In Two Phase Experiment---%

Total_Pressure_Loss = Total_Pressure_Loss_single+Total_Pressure_Loss_two;

%---Net Pressure---%

Net_Pressure = P_pump_generation-Total_Pressure_Loss;

plot(V_pump,Net_Pressure) %plots graph

ylim([41.67 60.4]) %limits y-axis

xlabel('Applied Voltage (V)'); %labels x-axis

ylabel('Net Pressure (Pa)'); %labels y-axis

title('Net Pressure With Varying Voltages'); %labels title
```

Evaporator Power Input and Condenser Length:

```
%---Code Written by: Darien Nate Khea, Date Written: 10/11/2015---%

%---Evaporator Calculations---%

m_dot = [2.43*10^-6:1.215*10^-6:2.43*10^-5]; %Desired mass flowrate range
[kg/s] (0.1 mL/min:0.05 mL/min:1 mL/min)

lat_heat_R123 = 170.2*10^3; %Latent heat of R123 [J/kg]

vap_q = 0.99; %Vapor Quality [dimensionless]

Q_evaporator = m_dot.*lat_heat_R123*vap_q; %Heat Transfer for Evaporation [W]

%---Condenser Calculations---%

D_condenser_i = 4.572*10^-3; %Diameter of condenser inlet [m], 0.18"

D_condenser_o = 4.572*10^-3; %Diameter of condenser outlet [m], 0.18"
```

```matlab
r_condenser_i = D_condenser_i/2; %Radius of condenser inlet[m]

r_condenser_o = D_condenser_o/2; %Radius of condenser outlet [m]

a_condenser_i = (pi*(D_condenser_i)^2)/4; %Area of condenser inner [m^2]

a_condenser_o = (pi*(D_condenser_o)^2)/4; %Area of condenser outer [m^2]

%---Heat Transfer Coefficient of R123 liquid phase---%

G_condenser = m_dot./(a_condenser_i); %Mass flowrate flux of liquid in
condenser [kg/s-m^2]

mu_liquid_R123 = 4.25*10^-4; %Viscosity of saturated liquid in condenser [Pa-
s] -Approximation-

k_R123_liq = 0.077; %Thermal conductivity of saturated liquid R123 [W/m-
Kelvin]

C_p_R123 = 729.4; %Specific heat of R123 [J/(kg-Kelvin)]

Pr_liquid = (C_p_R123*mu_liquid_R123)/(k_R123_liq); %Prandtl number of
saturated liquid R123 [dimensionless]

h_l =
0.023.*(((G_condenser.*D_condenser_i)./mu_liquid_R123).^0.8)*(Pr_liquid.^0.4)
.*(k_R123_liq/D_condenser_i); %Heat Transfer Coefficient for liquid phase
[W/(m^2-Kelvin)]

%---Heat Transfer Coefficient of R123 two phase inlet---%

p_sat = 91; %Saturated pressure of R123 [kPa]

p_crit = 3668; %Critical pressure of R123 [kPa]

p_star = p_sat/p_crit; %Ratio of pressures [dimensionless]

h_two_i = h_l.*(((1-vap_q)^0.8+(((3.8*(vap_q)^0.76)*(1-
vap_q)^0.04)/(p_star)^0.38))); %Heat Transfer Coefficient for two phase
[W/(m^2-Kelvin)]

%---Heat Transfer Coefficient of R123 two phase outlet---%

vap_q_o = 0.01;

h_two_o = h_l.*(((1-vap_q_o)^0.8+(((3.8*(vap_q_o)^0.76)*(1-
vap_q_o)^0.04)/(p_star)^0.38))); %Heat Transfer Coefficient for two phase
[W/(m^2-Kelvin)]

k_ss = 0.014*10^3; %Conductivity of stainless steel [W/m-k]

%---Average Heat Transfer Coefficient of R123 inlet/outlet---%
```

```matlab
h_avg = (h_two_i+h_two_o)/2; %Average Heat Transfer Coefficient for two phase
[W/(m^2-Kelvin)]

%---Based on highest mass flow rate (1 mL/min), heat needed for evaporator is
~4.1 W---%
%---Based on heat needed for evaporator/condenser for full phase change:---%
%---Length of condenser is ~ 6.61 in. or 0.168 m---%
%---Putting a safety factor of 2 should increase the overall condenser
%length to ~13.2 in. or 0.335 m---%
```

Differential Pressure Transducer:

VALIDYNE ENGINEERING

DP103

Ultra Low Range
Wet-Wet
Differential Pressure
Transducer

AC Output

Features

☐ **Full Scale Differential Pressure Ranges as Low as ±0.008 psid**

☐ **High Line Pressure Capability**

☐ **Wet-Wet Differential**

☐ **Equal Pressure Inlet Volumes**

☐ **Low Acceleration Sensitivity**

☐ **Field Replaceable Sensing Diaphragms**

Description

The Validyne DP103 is designed for exceedingly low differential pressure measurement applications where high accuracy is required under rough physical conditions. With full scale ranges down to –0.008 psid (–0.56cm H₂O), this instrument is being used in the measurement of very low flow rates of gases where symmetrical pressure cavities are required for dynamic response. It is also used in very small leak detection and pressure null detection systems.

Applications involving corrosive liquids and corrosive gases are easily handled as all surfaces exposed to the media are corrosion resistant steel. Overpressure as high as 100 psid will not destroy the sensing diaphragm and with recalibration the instrument may continue to be used.

Used with a typical Validyne carrier demodulator, –10Vdc output may be obtained for a pressure of –0.008 psid. The transducer may be located 1000 feet or more from the electronics with no problem.

Specifications

Standard Ranges:	–0.008 to –12.5 psid FS See Diaphragm Selection Chart on the following sheet.
Accuracy*:	–0.25% Full Scale
Hysteresis:	0.1% pressure excursion
Overpressure:	–200% Full Scale with less than 0.5% Full Scale Zero Shift
Overpressure Limit:	15 psi for -26 and below 100 psi for -28 and above
Line Pressure:	100 psig, less than 1% Zero Shift
Inductance:	20mH nominal, each coil
Zero Balance:	☐ –5mV/V at rated excitation
Excitation:	
Rated:	5 Vrms at 5kHz
Limit:	30 vrms at 3kHz 1 to 20 kHz with 20 mh coils
Sensitivity:	20mV/V for Full Scale, nominal
Pressure Media:	Corrosive fluids, compatible with 410ss, Inconel, and Buna N O-Rings.**
Temperature:	
Operating:	-65 to 250℉
Specified:	0 to 160℉
Thermal Zero Shift:	1%FS/100℉ typical
Thermal Sensitivity Shift:	5%/100℉ typical
Pressure Cavity Volume:	35X10⁻³ cubic inch (.57 cc)
Volumetric Displacement:	3 X10⁻³ cubic inch (.057 cc)
Pressure Connection:	1/8-27 NPTF
Electrical Connection:	Bendix PT06A-106S (SR) or equivalent, 10ft. cable provided
Size:	1.25☐X 4☐X 4.375☐
Weight:	39 ounces (1.11 Kg)
Replacement Diaphragms:	Order P/N 8-XX Diaphragm Dash Number from selection chart on the following sheet.

*Includes the effects of Linearity, Hysteresis, and Repeatability.
**See Ordering Information on the following sheet for available options.

Installation Drawing

Diaphragm Selection Chart
Use this chart to specify transducer diaphragm range.

Pressure Range Chart

Range Dash No.	PSI	IN HG	IN H₂O	KPA	TORR	CM H₂O
	0.003	0.006	0.09	0.022	0.17	0.22
06	0.005	0.010	0.14	0.035	0.26	0.35
08	0.008	0.016	0.22	0.055	0.41	0.56
10	0.0125	0.25	0.35	0.086	0.65	0.88
12	0.020	0.041	0.55	0.14	1.03	1.40
14	0.032	0.065	0.89	0.22	1.65	2.25
16	0.05	0.102	1.40	0.35	2.58	3.50
18	0.08	0.16	2.22	0.55	4.14	5.60
20	0.125	0.25	3.5	0.86	6.5	8.80
22	0.20	0.41	5.5	1.40	10.3	14.0
24	0.32	0.65	8.9	2.2	16.5	22.5
26	0.50	1.02	14.0	.5	25.8	35.0
28	0.80	1.6	22.2	5.5	41.4	56.0
30	1.25	2.5	35.0	8.6	65.0	88.0
32	2.0	4.1	55.0	14.0	103.0	140.0
34	3.2	6.5	90.0	22.0	165.0	225.0
36	5.0	10.2	140.0	35.0	258.0	350.0
38	8.0	16.0	222.0	55.0	414.0	560.0
40	12.5	25.0	350.0	86.0	650.0	880.0

To order replacement diaphragms, specify:

Model code and Range Dash No.

How To Use The Diaphragm Selection Chart

First, select the appropriate engineering units desired (PSI, IN HG, IN H₂O, KPA, TORR, or CM H₂O). Find the desired full-scale pressure range in this column. Then, note the corresponding **Range Dash Number** in the far left column. When ordering, use this number to specify the -XX- in the part number (See "Ordering Information")

Example: To obtain a 2.22 H₂O transducer, select a -18 Range Dash Number. This transducer may be calibrated from 0 H₂O to any full-scale pressure range between 1.40 and 2.22 H₂O.

If the pressure range desired falls between the ranges listed, use the Range Dash Number for the next higher range.

Example: To obtain a .10 PSI transducer, select a -20 Range Dash Number. This transducer may be calibrated from 0 PSI to any full scale pressure range between .08 and .125 PSI, including 0 to 0.10 psi.

Using the **Pressure Range Chart** assures that the transducer model selected will meet all performance specifications.

Ordering Information
For Transducers, specify part numbers as follows:

Pressure Range
Two-Digit Range Dash Number
See the Diaphragm selection Chart.

Temperature Range
S = 0 to 160 F (STD)

Sensor Material
4 = 410 Stainless Steel (STD)

DP103 – XX – N – 1 – S – 4 - D

O-Rings

N	=	Buna-N (STD)
E	=	Ethylene Propylene
V	=	Viton-A
S	=	Silicone
T	=	Teflon
		(2 psi & above)

Electrical Connectors

1	=	PTA06A-10-6S Bendix (STD)
2	=	PT06E-10-6S Bendix
3	=	WK-4-21 C-1/4, Cannon
4	=	WK-4-22 C-1/4, Cannon
7	=	NONE, Cable Ends Pigtalled
8	=	NONE, Wire Leads Pigtalled

Cable Length		Cable Type
A =	1 FT	Belden 8434
B =	18 IN	Belden 8434
C =	5 FT	Belden 8434
D =	10 FT	Belden 8434
E =	15 FT	Belden 8434
F =	25 FT	Belden 8434
G =	50 FT	Belden 8434
H =	100 FT	Belden 8434
K =	As Specified	4 leads 24 GA
L =	As Specified	Belden 8434

Flow Meter:

SENSIRION
THE SENSOR COMPANY

SLQ-HC60
Milliliter Flow Meter for Hydrocarbons

- Maximum flows up to 80 ml/min
- Sensitive to lowest flows
- Straight flow path, no moving parts
- Fast response time: < 50 ms
- Optimized for hydrocarbons

1   Introduction SLQ-HC60

The SLQ-HC60 Liquid Flow Meter enables fast, non invasive measurements of liquid flow up to 80 ml/min. This product line is especially suited for process monitoring applications in automation technology which require high sensitivity in the milliliter range. It is suited for use with almost all hydrocarbons, as for example, alcohols, oils, gasoline, diesel, etc. and many other chemicals. Excellent chemical resistance is ensured: The flow path of the SLQ-HC60 Liquid Flow Meters is formed by a simple, straight glass capillary. This Swiss made, non invasive flow meter is based on Sensirion's patented CMOSens® Technology (US Patent 6,813,944 B2). An internal fourth generation MEMS sensor chip combines a thermal high precision sensor element with amplification circuits and digital intelligence for linearization and temperature compensation on one single microchip – the product's core element.

2   Sensing Performance

In Table 1 the flow sensor's performance for use with Isopropyl Alcohol (IPA) is given. For other hydrocarbons the values will be slightly different as the performance depends on the medium used. Due to the optimized output signal the repeatability is nearly constant over a wide flow range. The repeatability depends on the integration time[a] of the analog signal acquisition. Longer integration time leads to better repeatability of the flow measurement (see table 1). The temperature compensation is optimized for use with IPA and shows very good performance for most hydrocarbons and other media.

Table 1: Model specific performance of SLQ-HC60 for IPA (all data at 20°C, 1 bar$_{abs}$ unless otherwise noted)

Parameter	Condition	SLQ-HC60	Units
Maximum Flow Rate	Best Performance	80	ml/min
	Reduced Performance	100	
Repeatability[b] (whichever is greater)	0.2 sec integration time	1.5	% m.v.
		0.2	% F.S.
	2 sec integration time	1	% m.v.
		0.07	% F.S.
Flow Detection Response Time		< 50	ms
Accuracy[c]		10	% m.v.
Response Time On Power-Up		120	ms
Mounting Orientation Sensitivity[d]	For IPA	0.25	ml/min
Operating Temperature	Temperature Compensated	+10...+40	°C
	Functional	+0 ... +55	°C
Ambient storage Temperature	(empty flow channel)	-10...+60	°C

---

[a] This refers to the time over which the analog acquisition device averages the input signal. Refer to the datasheet of your device.

[b] For medium IPA using 1 σ standard deviation of consecutive flow measurements.

[c] With IPA, 2.5-80 ml/min, after conversion of the Vout signal via the exponential relation. See section 3.1

[d] Normal position: Horizontal Flow channel, connector horizontally.

SENSIRION
THE SENSOR COMPANY

3   Output Signal and Media Compatibility

3.1 Output Signal

The SLQ-HC60 flow meter comes with an analog output (0...10V). Depending on the media used, the output will be about 5 Volt at zero flow. For positive flow rates the output signal increases logarithmically[a] with the flow rate for IPA (see figure 1). This signal characteristic has the advantage that the flow meter can be used at various flow rates with a constant relative error and makes measurements for a wide spectrum of liquids possible.
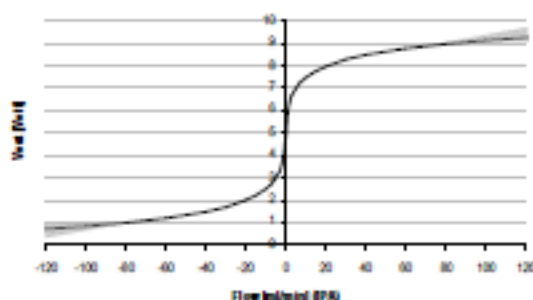

Figure 1: Sensor Signal for IPA

3.2 Signal for Other Media

For other media but IPA the form of the sensor signal will differ slightly as is demonstrated in figure 2. When using the sensor with other media but IPA, ask Sensirion for advice on how to handle the sensor signal to suit your requirements.

Because of the drastically different sensor response the sensor is not suited for use with water or aqueous solutions.

3.3 Maximum Flow Rate for Common Media

Due to the measurement principle, the thermal properties of the medium determine the sensor characteristics and the dynamic range of the device. For most hydrocarbons and most other media this range extends to about 80 ml/min. With reduced performance even rates of 100 ml/min or higher can be reached for some media. For low viscosity (< 1 centipoise) media the dynamic range can be limited by turbulence.

The dynamic ranges for various media are given in Table 2. For other media similar values can be expected.

Attention: If unsure about your medium please contact Sensirion for assistance.

Conversion: Signal to Flow (for positive flow rates)[a]

$$\text{Flow[ml/min]} = (\text{Exp}[(\text{Vout}-5)/0.729]-1)/3$$
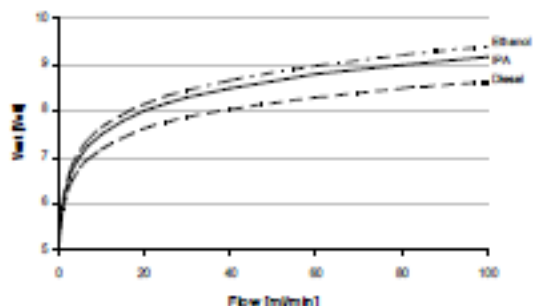$$= 1/3 * (e^{(\text{Vout}-5)/0.729}-1)$$

Figure 2: Sensor Signal for Various Media

Table 2: Examples for common media

Medium	Maximum Flow Rate	Units
IPA	80 (100[b])	
Ethanol, Methanol, Gasoline	~50	
Acetone	~40	ml/min
Diesel, Petroleum, Veg. Oils	80 (100[b])	
Silicon Oil, Ether	< 100	

---

[a] The flow rate for IPA is given by Flow[ml/min] = (Exp[(Vout-5)/0.729]-1)/3 for positive flow rates, i.e. above 5V. For negative flow rates the signal is symmetric: Flow[ml/min] = - (Exp[(5-Vout)/0.729]-1)/3. In Excel or when programming one can use the following formula for the full flow range: Flow[ml/min] = SIGN(Vout -5)*(EXP[SIGN(Vout -5)*(Vout -5)/ 0.729]-1)/3 where SIGN is -1 if the argument is negative and +1 if the argument is positive.

[b] At reduced requirements on accuracy (repeatability for other media but IPA) and exchangeability of sensors.

3.4 Exchangeability

Every SLQ-HC60 is calibrated for IPA. This makes the sensors also exchangeable for use with other media, meaning that once the sensors are characterized for a particular medium the same values can be used for further sensors. Depending on the media, variations between sensors of 6– 20% are typical.

4 Cleaning

Due to the measurement principle the sensor is sensitive to deposits on the inside of the sensor's capillary. Especially when changing from one liquid to another sufficient cleaning steps have to be performed to avoid non-soluble remainders on the capillary wall. Inadequate cleaning can lead to an offset and low repeatability. The cleaning procedure has to efficiently remove contaminations from the borosilicate glass surfaces. This is the material which is used for the straight flow channel inside the flow meter.
Any form of mechanical cleaning has to be avoided. This will easily damage the internal capillary.

## 5 Electrical and Mechanical Specifications

5.1 Electrical Specifications

Table 2: DC Characteristics.

Parameter	Conditions	Min.	Typ.	Max.	Units
Power Supply DC, VDD		16	24	26	V
Operating Current	V_{DD} = 24 V ⎓ , no load		3	4	mA
Analog Out Voltage Range		0		10	V
Load at Analog Out		10		∞	kΩ
Capacitive Load at Analog out				Tbd	pF

5.2 Electrical Connector and Pinout

Connector Type: Lumberg Pico (M8) male, 8-pole, threaded lock.

Pin	Function	Connect to	Color (pigtail cable)
1	Power Supply 24V	(+) of Power Supply	white
2			brown
3		Do not use.ª	green
4			yellow
5			grey
6	Analog Out 0-10 V	(+) of Signal Acquisition	pink
7	GND	Connect to ground\(–) of Power	blue
8	GND	Supply and Signal Acquisition	red
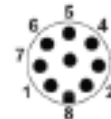
Note: Pins 7 and 8 have to be connected to ground of the Power Supply and the Signal Acquisition. Pins 2-5 are used in the calibration procedure, they have no functionality in normal use. Pins 2-5 cannot be used "as" the ground; they are not connected with Pins 7 and 8 inside the sensor.

5.3 Fluidic Connections

The repeatability of the measurement depends on a laminar flow of the liquid. Especially with low viscosity media improper connections to the sensor can unnecessarily reduce the maximum flow rate. Tubing with an inner diameter of less than 1.8 mm should be avoided. Make sure that the tubing has been cut properly.

5.4 Mechanical Specifications and Pressure Rating

Table 3: Mechanical Specifications and Pressure Rating

| Parameter	SLQ-HC60
Fluid Connector Standard (Fittings)	¼-28 flat bottom port for 1/8", 3mm OD tubing
Wetted Materials:	
• Internal Sensor Capillary Material	Duran® (borosilicate glass 3.3)
• Fitting Material	100% PEEK™ (polyetheretherketone)
• Additional Sealing Material	Tefzel® (ETFE)
Overpressure Resistance	3 bar
	45 psi
Maximum Pressure Drop (at 80 ml/min flow rate for IPA)	40 mbar
Internal Sensor Capillary, Inner Diameter	1.8 mm
Protection Class	IP 65
Total Mass	53 g

Attention	
Mechanical shocks and connecting to the fittings with excessive force can lead to stress on the internal thin walled glass capillary and can cause it to break. Test for leakage after every time new connections are made. Refer to Handling Instructions for precise information.	**!**

6   Physical Dimensions
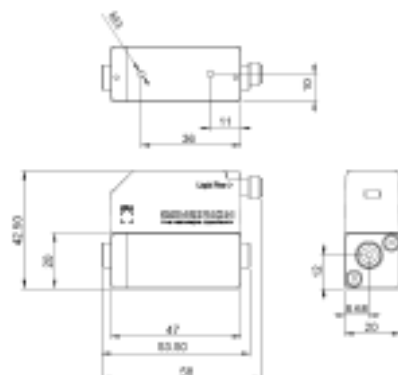
7   Ordering Info

The SLQ-HC60 can be ordered in the Flow Meter Kit at quantities up to 3 units. The Flow Meter Kit contains the sensor, the suitable connecting cable, a set of compression fittings for 1/8" OD tubing and a set of various barb connectors for easy setup for testing.

When ordering the SLQ-HC60 alone without the Flow Meter Kit it comes only with the cables but without fitting material.

Product	Article Number
Flow Meter Kit SLQ-HC60	1-100870-01
SLQ-HC60	1-100605-01